Chapter 5
Nanografting: A Method for Bottom-up Fabrication of Designed Nanostructures

Tian Tian, Zorabel M. LeJeune, Wilson K. Serem, Jing-Jiang Yu, and Jayne C. Garno

Abstract Nanografting is a scanning probe-based technique which takes advantage of the localized tip-surface contact to rapidly and reproducibly inscribe arrays of nanopatterns of thiol self-assembled monolayers (SAMs) and other nanomaterials with nanometer-scale resolution. Scanning probe-based approaches for lithography such as nanografting with self-assembled monolayers extend beyond simple fabrication of nanostructures to enable nanoscale control of the surface composition and chemical reactivity from the bottom-up. Commercial scanning probe instruments typically provide software to control the length, direction, speed and applied force of the scanning motion of a tip, analogous to a pen-plotter. Nanografting is accomplished by force-induced displacement of molecules of a matrix SAM, followed immediately by the surface self-assembly of *n*-alkanethiol *ink* molecules from solution. Desired surface chemistries can be patterned by choosing SAMs of different lengths and terminal groups. By combining nanografting and designed spatial selectivity of *n*-alkanethiols, in situ studies provide new capabilities for nanoscale surface reactions with proteins, nanoparticles or chemical assembly. Methods to precisely arrange molecules on surfaces will contribute to development of molecular device architectures for future nanotechnologies.

Keywords Nanografting · Scanning probe lithography · Nanolithography · Self-assembled monolayer · Atomic force microscopy · Nanopatterning · Alkanethiols · Protein patterning · DNA · Porphyrins · Nanoparticles · Nanostructures

Abbreviations

AFM	Atomic force microscope
APDES	Aminopropyldiethoxysilane
bps	Base pairs
BSA	Bovine serum albumin
C8DMS	Octyldimethylmonochlorosilane

J.C. Garno (✉)
Department of Chemistry, Louisiana State University, Baton Rouge, LA 70803, USA
e-mail: jgarno@lsu.edu

A.A. Tseng (ed.), *Tip-Based Nanofabrication*, DOI 10.1007/978-1-4419-9899-6_5,

C10	Decanethiol
C12	Dodecanethiol
C18	Octadecanethiol
CAM	Computer-assisted manufacturing
DNA	Deoxyribonucleic acid
DPN	Dip-pen nanolithography
DPP	5,10-diphenyl-15,20-di-pyridin-4-yl-porphyrin
dsDNA	Double-stranded DNA
EDC	1-ethyl-3-(3-dimethylaminopropyl) carbodiimide hydrochloride
EG	Ethylene glycol
GIXD	Grazing incidence X-ray diffraction
IgG	Immunoglobulin G
MBP	Maltose binding protein
MCH	6-mercaptohexan-1-ol
16-MHA	16-mercaptohexadecanoic acid
MHP	*n*-(6-mercapto hexyl) pyridinium bromide
MPA	3-mercaptopropionic acid
11-MUA	11-mercaptoundecanoic acid
11-MUD	11-mercaptoundecanol
NEXAFS	Near-edge X-ray absorption fine structure spectroscopy
NHS	N-hydroxysuccinimide
NPRW	Nanopen reader and writer
ODT	Octadecanethiol
OTS	Octadecyltrichlorosilane ($CH_3(CH_2)_{17}SiCl_3$)
SAMs	Self-assembled monolayers
SpA	Staphylococcal protein A
SPL	Scanning probe lithography
ssDNA	Single-stranded DNA

5.1 Introduction

Scanning probe lithography (SPL) enables bottom-up fabrication of nanostructures on surfaces for producing features with nanoscale dimensions. Methods using the probe of an atomic force microscope (AFM) have been used to fabricate sophisticated architectures at the molecular level with high spatial precision. A number of AFM-based approaches for SPL have been developed such as nanoshaving [1–5], nanografting [6–9], dip-pen nanolithography (DPN) [10, 11], NanoPen Reader and Writer (NPRW) [12–14], catalytic probe lithography [15–17], and bias-induced nanolithography [18, 19]. This chapter will focus specifically on the capabilities of nanografting for inscribing patterns of diverse composition from the bottom-up, to produce complicated surface designs with well-defined chemistries. Nanografting provides a versatile tool for generating nanostructures of organic and biological molecules, as well as nanoparticles. Protocols of nanografting are accomplished in liquid media, providing a mechanism for introducing new reagents for successive in situ steps for 3-D fabrication of complex nanostructures.

Nanografting was first introduced in 1997 by Xu, et al. and is accomplished by applying mechanical force to an AFM probe to generate nanostructures within a matrix film [8]. The molecules to be patterned are dissolved in the imaging media, and the substrates are precoated with a protective layer to prevent nonspecific adsorption of molecules throughout areas of the surface. When the tip is operated in liquid media under low force (less than 1 nN), high resolution characterizations of surfaces can be acquired in situ. When the force applied to the probe is increased to a certain displacement threshold the tip becomes a tool for surface fabrication. The exquisite resolution achieved with nanografting is mainly attributable to liquid imaging. When AFM experiments are conducted in liquid media, very low force can be used to accomplish imaging or nanofabrication. The geometry of the apex of the probe is preserved by operating at low forces, because liquid media serves to minimize the strong capillary forces of attraction that cause adhesion between the tip and sample [20, 21].

5.1.1 General Procedure for Nanografting

The basic steps for nanografting are presented in Fig. 5.1. In the first step, the surface of a self-assembled monolayer (SAM) prepared on a Au(111) substrate is imaged using low force in liquid media that contains the molecule or nanomaterial to be patterned. When the tip is operated at low force the surface is not damaged or altered by the scanning probe (Fig. 5.1a). A suitable flat area can be selected for inscribing

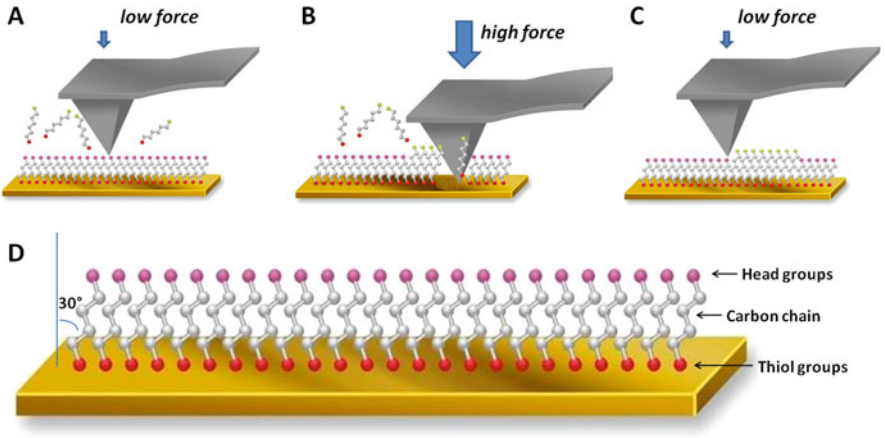

Fig. 5.1 Steps for producing patterns of *n*-alkanethiols with nanografting by changing the mechanical force applied to the AFM probe. The process is accomplished under liquid imaging media containing the molecules to be patterned. (**a**) Characterization is accomplished when the tip is operated at low force; (**b**) patterns are nanografted when the force is increased to a certain displacement threshold; (**c**) returning to low force, the patterns are characterized in situ. (**d**) Model of an *n*-alkanethiol self-assembled monolayer

patterns that has few defects or contaminants. Next, the tip is raster scanned across the surface using higher force to sweep away selected regions of the matrix SAM. During the fabrication step (Fig. 5.1b), fresh molecules from solution bind to the exposed areas of the substrate immediately following the pathway of the scanning probe to produce nanopatterns. Finally, the pattern that was grafted can be characterized in situ by returning to a low force for nondestructive imaging (Fig. 5.1c). Patterning and imaging are accomplished in situ with the same AFM tip, within a few minutes or less. The entire process can be automated to reproducibly write multiple patterns [22, 23].

A key requirement for nanografting is to determine the necessary amount of force for cleanly removing local areas of the matrix monolayer without damaging the tip. To find the appropriate force, one can monitor surface changes in situ while successively increasing the load applied to the tip. As the force is gradually increased at small increments, images will clearly show changes in surface morphology at a certain threshold. The optimum force must be derived for each experiment for several reasons. At the nanoscale, the actual geometry of tips is never identical and thus the sharpness will vary from probe to probe. Also, different amounts of force are necessary for matrix layers of different thicknesses or compositions. The requisite force needed for imaging in various liquid media will change according to dissolution parameters, for example the forces required for nanografting in aqueous media are not the same as for ethanolic media. For each system, the amount of force to be applied for fabrication must be determined experimentally.

5.1.2 Applicability of Nanografting for In Situ Studies

Nanografting can achieve high spatial resolution. The length, size and shape of patterns can be controlled precisely, achieving an edge resolution of 1 nm and line widths of 10 nm or less, depending on the dimensions of the probe. The head groups of grafted structures can be selected by choosing different molecules, such as aldehydes, carboxylates, thiols, amines, and others. The thickness of the patterns can be designed by choosing the carbon backbone of the matrix and nanografted molecules. Nanografting enables in situ reactions to be studied locally under dilute conditions [24]. Time-lapse AFM images can be acquired at selected intervals to view reaction kinetics for conditions that occur over time scales of minutes to hours. A range of different molecules and nanomaterials have been patterned with nanografting, examples will be described in this chapter for *n*-alkanethiol SAMs [14, 25], metals [26], nanoparticles [27], porphyrins [28], proteins [29–32] and DNA [33].

Among the most significant contributions of scanning probe studies with nanografting are the possibilities for studying step-wise surface reactions in real time with a molecular-level view. Imaging in liquid media provides a means for exchanging liquids to introduce new reagents in successive steps to build nanostructures from the bottom-up. To date, the primary examples that have been reported demonstrate nanografted patterns of *n*-alkanethiol SAMs, often as a foundation for

attaching other molecules and nanomaterials. Further chemistries for nanografting experiments are likely to be extended to other types of surface binding motifs, such as phosphonic acids on metal substrates [34]; siloxane binding, pyridyl-[28] or thiol-[35] functionalized porphyrins, thiolated proteins [36, 37], thiolated DNA [33] or peptides and other types of surface linkers.

5.2 Patterning *n*-Alkanethiol Self-Assembled Monolayers (SAMs by Nanografting)

As a starting point, SAMs of *n*-alkanethiols prepared on gold substrates provide a model system for nanografting experiments. Thiol end groups furnish a functional handle for surface attachment, mediated by sulfur-gold chemisorption. The self-assembly process and surface structures of *n*-alkanethiols on Au(111) have been previously described [38, 39]. The carbon backbones of the molecules consist of tilted alkane chains (Fig. 5.1d), the lengths of which can be designed to define the thickness of the matrix areas and nanografted patterns. For *n*-alkanethiol SAMs, chain lengths ranging from 2 to 37 carbons have been nanografted successfully. The head groups of *n*-alkanethiols provide a way to attach other molecules and nanomaterials with spatial selectivity; for example, experiments can be designed to define patterned sites for specific adsorption of proteins, nanoparticles or DNA, within a matrix monolayer that resists binding of molecules or nanomaterials.

Nanopatterns of octadecanethiol (18 carbon backbone or C18) were nanografted side-by-side within a matrix SAM of decanethiol (10-carbon backbone or C10) as shown in Fig. 5.2a [8]. The square patterns measured 0.88 nm taller than the matrix.

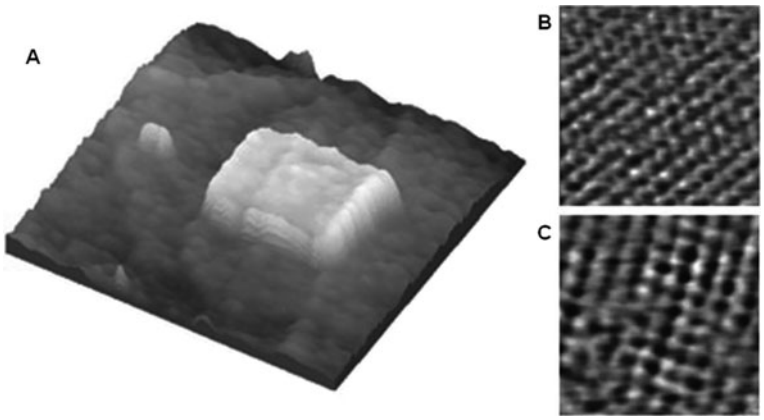

Fig. 5.2 Patterns of *n*-octadecanethiol were nanografted within a matrix monolayer of decanethiol. (**a**) AFM topography view (130 × 130 nm^2); (**b**) zoom-in view of the pattern surface (5 × 5 nm^2); (**c**) Zoom view from an area of the C10 matrix (5 × 5 nm^2). (Reprinted with permission from Ref. [8]. Copyright © American Chemical Society)

The dimensions of the smaller feature are 3 nm × 5 nm, in which approximately 60 thiol molecules were grafted. The size of the larger nanopattern is 50 × 50 nm^2. Zoom-in views of both the nanografted pattern of C18 and the C10 matrix are shown by in situ AFM topography images in Fig. 5.2b, c, respectively. The molecularly resolved images show that molecules within the nanopatterns display a periodic $(\sqrt{3} \times \sqrt{3})$ R30° lattice, thus the packing arrangement of thiols is preserved for alkanethiol nanostructures produced by nanografting.

Nanografted structures can be erased and rewritten in situ by exchanging the imaging media with different molecular adsorbates for patterning. Results for writing two parallel line patterns of octadecanethiol within a decanethiol matrix with a distance of 20 nm between patterns were shown by Xu and others [9]. One of the lines was erased by replacing the liquid imaging media with a solution of decanethiol and scanning at high force over one of the C18 patterns to replace the previous nanostructure with C10 molecules. After the line pattern was "erased" the imaging media was exchanged again to introduce a fresh solution of C18SH molecules to graft a line pattern spaced 65 nm from the previous pattern. Accomplishing this experiment required a scanning probe microscope with high stability, however this clearly demonstrates the flexibility for introducing and exchanging reagent solutions for multiple synthetic steps when imaging with AFM in liquids.

Different shapes and molecular components can be patterned by nanografting. Several letter patterns that spell the acronym "AFM" are shown in Fig. 5.3 that are terminated with carboxyl head groups. The line widths of the letter patterns are less than 10 nm, indicating that the very sharp AFM probe was not damaged by the physical process of scanning with the tip under high force. Although the AFM images of the patterns were captured after the writing process, we can still resolve the ultra-fine distinctive features of the matrix monolayer of decanethiol, resolving the characteristic details of an alkanethiol SAM landscape such as pinholes, scars, molecular

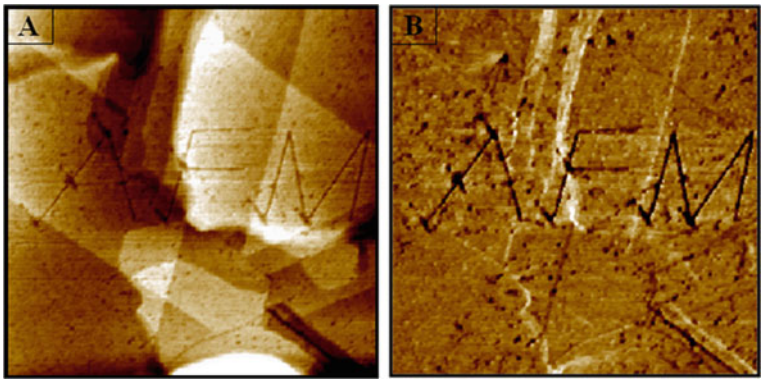

Fig. 5.3 Nanografted letters of 3-mercaptopropionic acid written within a decanethiol matrix SAM. (**a**) Topographic image (600 × 600 nm^2); (**b**) concurrent lateral force image of the same area

island vacancies [40] and overlapping gold terrace steps. The patterns are composed of 3-mercaptopropionic acid written within a decanethiol matrix. The difference in terminal chemistry is clearly distinguishable in the simultaneously acquired lateral force AFM image of Fig. 5.3b. Lateral force images do not show changes in height, instead the image contrast reveals nanoscopic differences in frictional and adhesive forces between the tip and surface. In this example, the tip-surface interactions are markedly different for the dark areas of the nanografted letters which are terminated with thiol head groups, as compared to the brighter areas of the surrounding methyl-terminated matrix SAM.

The simplicity of SAM preparation is another benefit of nanografting protocols. A matrix monolayer can be prepared by simply immersing a clean substrate into a dilute solution of *n*-alkanethiol in ethanol or sec-butanol for one or more hours. After a SAM film is formed on the metal substrate, the sample can be stored for several weeks in a solution of clean solvent, and often can be recycled and used for several experiments. Nanografted patterns can be engineered to incorporate diverse head group chemistries, such as methyl, alcohol, glycol, aldehyde, amide and carboxylate. Table 5.1 lists examples of thiol self-assembled monolayers which have been patterned using nanografting. Methyl-terminated SAMs of decanethiol or octadecanethiol have been commonly used as matrix monolayers for nanografting. Either ethanol or 2-butanol are most frequently used as solvents for liquid imaging. Patterns of diverse shapes, such as squares, rectangles and rings have been reported ranging up to 500 nm in size, with the dimensions of the smallest pattern measuring 3 nm $\times$ 5 nm.

5.2.1 Automated Nanografting

Beyond simple patterns of lines or rectangles, nanografting can be used to fabricate complicated designs with modern computer automation. The William Blake quotation "What is now proved was once only imagined" was nanografted with mercaptohexadecanoic acid by Cruchon-Dupeyrat, et al., using computer-assisted manufacturing (CAM) software [23]. The entire quotation was written in less than 20 s, inscribed within a 1.85 $\times$ 0.9 μm^2 area. Arrays of circles, squares, lines and even mouse ear designs were produced by automated nanografting of different functionalized alkanethiols by Ngunjiri and others [22]. A sophisticated example was demonstrated by Maozi Liu, et al. for nanografting the design of the University of California at Davis' seal with a 10 nm line resolution using an aldehyde terminated alkanethiol within a decanethiol SAM [25]. The design was patterned inside an 8 $\times$ 8 μm^2 area and was completed in 10 min.

The speed and ease of nanografting for AFM experiments has been greatly improved by advances in software for commercial instruments. Louisiana State University implemented nanografting experiments in physical chemistry laboratories starting in 2005 to teach and showcase the concepts of chemistry and nanoscience to undergraduate students [41]. Nanografted patterns can be produced

Table 5.1 Examples of thiol SAMs that have been successfully nanografted

Nanografted molecule	Pattern dimensions	Matrix film	Liquid media	References
1-hexanethiol	5.2 nm × 5.2 nm	Thiolated biotin SAMs	Ethanol	[32]
1-octadecanethiol	3 nm × 5 nm 50 nm × 60 nm	1-decanethiol	2-butanol	[8]
1-decanedithiol	100 nm × 100 nm	1-decanethiol	2-butanol	[61]
Dodecanethiol	300 nm × 300 nm	1,9-nonanedithiol	Ethanol	[86]
1-octadecanethiol	20 nm × 60 nm	1-decanethiol or 1-octadecanethiol	2-butanol	[9]
Docosanethiol	25 nm × 60 nm			
2-mercaptoethanol	75 nm × 100 nm			
16-mercapto-hexadecanoic acid	70 nm × 300 nm			
3-mercapto-1-propanoic acid	400 nm × 400 nm	$C_{11}(EG)_6$	Water	[73]
11-mercapto-1-undecanal	50 nm × 50 nm 100 nm × 100 nm	1-octadecanethiol	Decahydro-naphthalene	[62]
11-mercapto-undecanoic acid	Rings with diameter of 100 nm	1-octadecanethiol	Ethanol	[29]
1,8-octanedithiol	500 nm × 500 nm	Hexanethiol	Ethanol	[86]
6-mercaptohexan-1-ol	400 nm × 400 nm	$C_{11}(EG)_6$	Water	[73]
Biphenyl 4,4'-dithiol	100 nm × 100 nm	1-decanethiol	2-butanol	[61]
Mixed-*n*-alkanethiols	200 nm × 200 nm	1-decanethiol: 1-octadecanethiol =10:1	Ethanol or 2-butanol	[53]
10:1 ODT:decanethiol	200 nm × 200 nm	Hexanethiol	Ethanol,	[53]
$CF_3(CF_2)_9(CH_2)_2SH$	15 nm × 15 nm 300 nm × 300 nm	Dodecanol Mixed SAM matrices	2-butanol or poly-α-olefin oil	
1-octadecanethiol	70 nm × 50 nm 175 nm × 225 nm 20, 50, 100, 200 nm	Decanethiol Mixed SAMs	Ethanol, 2-butanol or hexadecane	[54]

within a few minutes and thus are an excellent venue for providing hands-on training for students. At present, scanning probe-based lithography is primarily used for laboratory research rather than as a tool for industry. Knowledge and experience in modern methods of surface measurements and analysis will be pivotal to the eventual transfer of the technology gained with academic nanoscience research to benefit industry. The latest advances in automation of scanning probe instruments enable new possibilities for educational modules for engaging students with modern and compelling course activities, such as with nanografting studies.

5.2.2 Evaluating the Tip Geometry with Nanografting

For both imaging and nanofabrication with an AFM probe, the shape of the apex of the tip is critical for high resolution. Nanografting provides a way to evaluate the shape of an AFM tip, to help discern if images show artifacts or represent the true shape of surface structures [42]. Line patterns of alkanethiol SAMs are first fabricated using nanografting with a single scan, and then imaged using the same tip. The tip size and tip-surface contact area can be derived from cursor profiles in AFM topography views. The shape of the apex of the tip can be reconstructed by imaging small surface features of nanografted SAMs with known dimensions. When the tip is engaged for a sweeping a single line pattern, the width of the trench or pattern provides a reliable estimate of the tip-surface contact area. Tips with multiple asperities produce multiple nanopatterns. This approach is especially helpful for identifying tips with multiple asperities that are difficult to characterize by other techniques.

5.2.3 Nanografted Patterns of n-Alkanethiols Furnish a Molecular Ruler

Since the dimensions of methyl-terminated *n*-alkanethiols have been well-established, the height and orientation of other molecules can be evaluated by nanografting experiments, by referencing the thickness of *n*-alkanethiols as an in situ molecular ruler. Methyl-terminated *n*-alkanethiols can be prepared reproducibly with predictable, well-defined surface structures, thus nanografted patterns furnish a reliable height reference for nanoscale measurements of film thickness. Self–assembled monolayers of *n*-alkanethiols spontaneously form hexagonally-packed crystalline layers upon adsorption to metal surfaces, with an intermolecular spacing of ∼0.5 nm [43]. The well-ordered packing of *n*-alkanethiol SAMs results from a strong affinity to the substrate through chemisorptive binding to produce a commensurate structure, and also from intermolecular chain-chain interactions of Van der Waals forces between the carbon backbones. Methyl-terminated *n*-alkanethiols form SAMs with a single thiol end group chemisorbed to Au(111) oriented in an upright configuration, with all-trans carbon chains. Studies conducted

using IR, near-edge X-ray absorption fine structure (NEXAFS) spectroscopy, and grazing incidence X-ray diffraction (GIXD) indicate that the alkyl chains of SAMs are tilted $\sim 30^{\circ}$ with respect to surface normal [44–47]. The consistency for preparing reproducible molecular structures of *n*-alkanethiols provides predictable dimensions as a means to study structures of other patterned molecules using side-by-side local measurements of height differences with AFM-based nanografting protocols [12, 48, 49].

By labeling the DNA 3′ end with a fluorophore and immobilizing it onto a gold surface through thiol modification of the 5′ end, a pH-driven DNA nanoswitch can be reversibly actuated. By cycling the solution pH between 4.5 and 9, a conformational change is produced between a four-stranded and a double-stranded DNA structure which either elongates or shortens the separation distance between the 5′ and 3′ ends of the DNA. The nanoscale motion of the DNA produces mechanical work to lift up and bring down the fluorophore from the gold surface by at least 2.5 nm and transduces this motion into an optical "on-and-off" nanoswitch. Nanografting was used to measure the thickness of the monolayers of thiolated "motor" DNA under changing pH conditions by Dongsheng Liu, et al., [50]. Before nanografting, a DNA SAM prepared on template-stripped gold surface was first imaged under low force (0.2–0.5 nN) in phosphate buffered saline (pH 4.5) containing 1 mM of 2-mercaptoethanol. The area for nanografting was repeatedly scanned at 4–5 Hz under higher forces (~30 nN) to scratch away the DNA SAM, creating a freshly exposed gold surface that was immediately grafted with a SAM of 2-mercaptoethanol. After nanografting, a wider scan area was characterized under low force. Changes in the thickness of the DNA film measured at pH 4.5 and 9 were attributed to differences in the electrostatic interactions between the tip and the DNA layer.

5.2.4 Evaluating Properties Such as Friction, Elastic Compliance or Conductivity of Nanografted Patterns

Friction mapping can be accomplished with AFM to provide useful information about the composition and chemical properties of a surface with nanoscale sensitivity. A systematic study of differences in molecular friction was accomplished in situ for nanografted patterns of different ω-functionalized *n*-alkanethiols by Joost te Riet et al., [51, 52]. Trace and retrace lateral force images were subtracted to reveal the net frictional forces to obtain quantitative frictional force measurements at the nanoscale. Images of nanografted patterns with fluorocarbon-, hydroxyl-, thiol-, amine- and acid- terminated head groups were obtained in 2-butanol under common conditions of load force and scan speed. The same cantilever was used for nanografting patterns and acquiring in situ images in liquid media. In each case, they observed that the friction of the nanografted patches was lower than that of the surrounding matrix SAM. However, nanografted patterns with functional head groups showed statistically higher friction values than nanografted patterns with

methyl groups. These observations were attributed to differences in topographical roughness of the nanografted patches, the amount of disorder and defects within the patterns, as well as surface composition.

Changes in molecular-level packing, molecule chain lengths, domain boundaries, and surface chemical functionalities in nanografted SAM nanopatterns can be sensitively characterized using force modulation imaging [53]. Size-dependent changes in elasticity were detected for test platforms of nanografted SAM patterns by Price, et al., [54]. Surface patterns of octadecanethiol (ODT) of designed sizes and shapes were nanografted into *n*-alkanethiol SAMs for studies of the local mechanical properties using force modulation imaging. Certain surface features such as the edges of the domains and nanostructures or desired chemical functionalities can be selectively enhanced in the amplitude images when the driving frequency of sample modulation is tuned to the resonance frequencies of the tip-surface contact [53]. By means of tuning the driving frequency of sample modulation to certain frequencies, the resonances at the tip-surface contact are activated to sensitively reveal characteristic contrast for surface changes in molecular-level packing, molecule chain lengths, domain boundaries, and surface chemical functionalities of SAM nanopatterns. These studies demonstrate that the resonance frequency of the tip surface contact vary according to dimensions of the nanostructures. Frequency spectra of the tip surface contacts were acquired for nanografted ODT structures, from which Young's modulus was calculated using continuum mechanics models.

An approach to study metal-molecule-metal junctions based on combining approaches for nanografting and conductive probe AFM was demonstrated by Scaini, et al., [55]. Patterns of alkanethiol molecules were nanografted within a SAM of alkanethiol molecules of different chain lengths for local measurements of charge transport at the molecular level. The approach enables relative determination of the differential resistance between two molecular layers in ambient conditions; however absolute transport measurements also depend on the nature of the AFM tip-molecule contact. The tunneling decay constants of alkanethiols were measured as a function of chain lengths for octanethiol, nonanethiol and decanethiol nanopatterns relative to a matrix SAM of octadecanethiol/Au(111).

5.3 Spatially Confined Self-Assembly Mechanism of Nanografting

Both the assembly mechanism and kinetics of certain surface reactions can be sterically changed by spatial confinement with nanografting. Nanografted patterns of *n*-alkanethiols exhibit higher coverage and two-dimensional crystallinity than the matrix SAMs [56]. During the process of nanografting, thiolated molecules self-assemble within a spatially confined environment. A transient nanoscopic area of the surface is exposed by the scanning probe, which is confined by the surrounding matrix and the probe. During the nanografting process, thiol molecules present in

the solution rapidly assemble onto the exposed nanometer-size area of gold substrate that is confined by the scanning tip and surrounding matrix SAM. Spatial confinement is considered to alter the pathway for the self-assembly process causing the initially adsorbed thiols to adopt a standing-up configuration directly within a nano-sized environment. The mechanism for conventional solution self-assembly occurs through a two-step process when bare gold substrates are immersed in thiol solutions, because the assembly of thiols takes place in unconstrained conditions. Initially a "lying-down" phase is spontaneously formed which subsequently transitions over time by rearrangement to a standing-up orientation [38]. In contrast, with nanografting the "lying-down" configuration is not possible because the area of the surface exposed is smaller than the molecular length, therefore the molecules assemble directly into an upright or standing orientation [57]. Self-assembly within the constrained areas proceeds with a faster reaction rate because the time lapse for a phase transition from lying-down to an upright configuration is bypassed. Thus, the kinetics of SAMs formed with nanografting occur more rapidly than during natural growth on unconstrained surfaces. The spatially confined environment was found to reduce the amount of disorder present in the resulting nanografted patterns, to produce SAMs which exhibit fewer scars or defects [51, 56].

5.3.1 Studies with Binary Mixtures of SAMs

A nanoengineering approach to regulate the lateral heterogeneity of mixed self-assembled monolayers was reported using nanografting and self-assembly chemistry [51]. Formation of segregated domains in mixed SAMs results from the interplay between reaction kinetics and thermodynamics. Considerable effort has been directed to investigate the impact of either reacting agents or surface reaction conditions such as concentration, temperature, thiol species and molar ratio of mixed components for achieving control of the resulting local domain structures. For example, kinetics-driven products for mixed SAMs with a near molecular-level mixing were favored during coadsorption of thiol mixtures at high concentration with elevated temperature [58]. Thermodynamics-driven layers of large segregated domains were observed after long immersion in dilute solutions and/or when the adsorbate chain length and termini were sufficiently different [59]. Nanografting provides additional control of the reaction mechanism for thiol self-assembly on gold, and thus affects the local domain structures that are produced from solutions of mixed SAMs.

The heterogeneity of mixed solutions of SAMs can be regulated by changing the speed of nanografting [57]. This was demonstrated both theoretically [60] and experimentally [57]. Monte Carlo simulations of nanografting were found to reproduce experimental observations concerning the variation of SAM heterogeneity with the speed of an AFM tip. Simulations by Ryu, et al. demonstrated that the faster the AFM tip displaced adsorbed molecules in a monolayer, the monolayers formed behind the tip became more heterogeneous, according to the amount of space and

time available for the formation of phase-segregated domains. By varying fabrication parameters of nanografting, the lateral heterogeneity can be adjusted to produce near molecular mixing or to form segregated domains ranging from several to tens of nanometers [51].

5.4 In Situ Studies of Polymerization Reactions via Nanografting

Beyond preparing monolayer patterns of ω-functionalized *n*-alkanethiols, multilayer nanostructures can also be generated by nanografting. Depending on the concentration of thiols in the imaging media, patterns with the thickness of a bilayer were shown to form spontaneously by nanografting SAMs of certain head group chemistries [12, 61]. This is mediated by self-polymerization of molecules which have reactive groups through coupling of headgroups. Under certain conditions of high concentration, the intermolecular interactions between molecules in solution predominate, to direct the vertical self-assembly of certain α, ω-alkanedithiols to produce bilayer patterns. For SAM patterns with methyl, hydroxyl, thiol, or carboxylic acid head groups, monolayer patterns were generated when nanografting in dilute ethanol or aqueous solutions. However, as the solution concentration was increased beyond a certain threshold, nanografted patterns were formed with thicknesses corresponding to a double layer for molecules with carboxylic acid head groups or with α, ω-alkanedithiols, as reported by Kelley, et al. [12]. Nanografted patterns with methyl or hydroxyl head groups were observed to exclusively form monolayer structures for a fairly wide range of concentrations that were tested.

Designed functional groups of *n*-alkanethiols were used to attach additional organic molecules to enable site-selective surface reactions for studies of polymerization reactions at the nanoscale [62]. In the first step, nanografting was used to produce 2D nanopatterns of methyl head groups in a matrix SAM with hydroxyl head groups. The nanopatterns were then used to further construct 3D nanostructures by successive steps of an in situ reaction with organosilanes. Jun-Fu Liu et al. demonstrated transfer of 2D nanopatterns to chemically distinct 3D nanostructures with different head groups. The scheme and results for pattern transfer are shown in Fig. 5.4. A nanografted rectangular frame of octadecanethiol was inscribed within a matrix SAM of mercaptoundecanol on a gold substrate. The pattern of a frame in Fig. 5.4b measured 0.7 ± 0.2 nm taller than the matrix monolayer, in agreement with the expected theoretical dimensions. After nanografting, the AFM liquid cell was rinsed three times with decahydronaphthalene to remove any residual thiols, then a solution of octadecyltrichlorosilane ($CH_3(CH_2)_{17}SiCl_3$ or OTS) was injected into the cell for several minutes. The trichlorosilanes from the liquid media reacted with the hydroxyl terminal groups of the surrounding matrix SAM of mercaptoundecanol to form a thicker layer. However, the frame patterns did not react with OTS since the nanografted pattern with methyl head groups provided an effective resist, as shown in Fig. 5.4c. After reaction with OTS the nanografted frame is shorter than

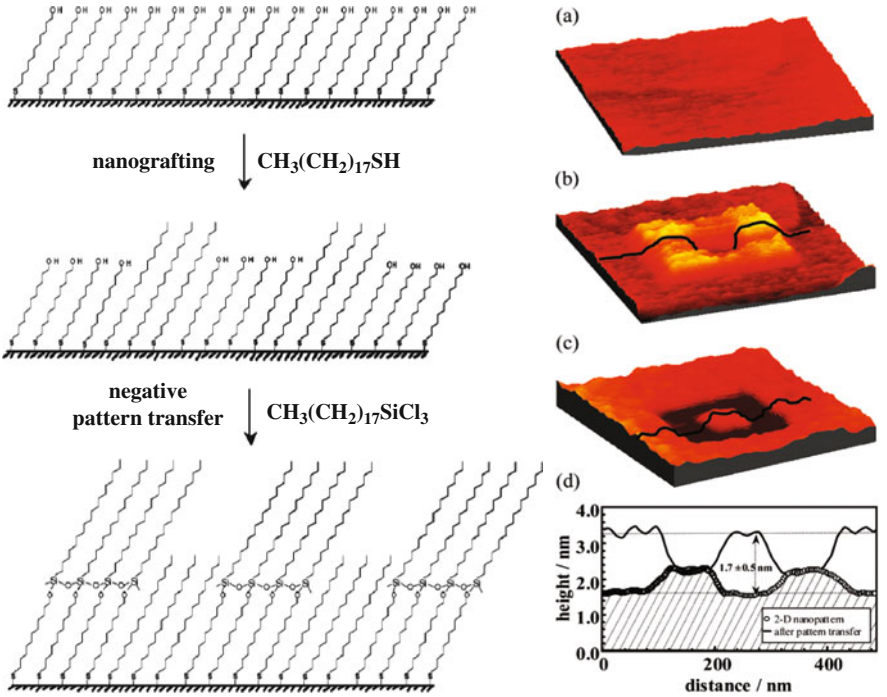

Fig. 5.4 Snapshots showing bottom-up assembly accomplished in situ with a polymerization reaction for attaching organosilanes to a hydroxyl-terminated SAM. (**a**) Initial view of a mercaptoundecanol monolayer formed on Au(111); (**b**) Nanografted frame of ODT; (**c**) Pattern is shorter than the matrix SAM after reaction with OTS; (**d**) representative cursor profile for lines in (**b**) and (**c**). (Reprinted with permission from Ref. [62]. Copyright © American Chemical Society)

the surrounding matrix film. The height changes at each step of the in situ reaction are shown with representative cursor profiles in Fig. 5.4d. The process was completed within a few minutes and the time duration for immersion in OTS was found to influence the height of siloxane structures.

Nanografting enables a critical first step for developing further protocols for designed surface reactions to construct hierarchical nanostructures with desired spacer lengths, composition and functionalities. The 2D patterns produced by nanografting provide a surface template for spatially directing the selective adsorption or binding of other molecules or nanomaterials in subsequent steps. Further examples will be presented in the next sections. The desired interfacial properties, such as lubricity, protein adhesion or resistance, and electron transfer, may be designed from the bottom-up by selection of various functional groups and designated architectures of the nanografted structures of metals, nanoparticles, protein or DNA.

5.5 Generating Patterns of Metals and Nanoparticles with Nanografting

Certain systems of metals and nanoparticles have been patterned successfully with AFM-based lithography. Nanopatterns of thiol-coated gold nanoparticles were prepared within a decanethiol SAM on Au(111) by scanning probe lithography [27]. To attach nanoparticles to gold surfaces via sulfur-gold chemisorption, surface-active gold nanoparticles were prepared with a shell of a mixed monolayer comprised of alkanethiol and alkanedithiol molecules. Local regions of a decanethiol SAM were shaved using an AFM tip under high force to expose the substrate in a solution containing nanoparticles. Unlike nanografting where surface assembly is immediate, the kinetics of larger nanomaterials such as gold nanoparticles were found to be slower and took place over longer time scales. Depending on the concentration, thiolated nanoparticles adsorbed onto the exposed areas uncovered by the AFM tip after several hours, and particles were not observed to bind to the surrounding matrix areas of the methyl-terminated decanethiol SAM. Gold nanoparticles attached to the gold substrate via sulfur-gold chemisorption. The outer shell of the nanoparticles was encapsulated with mixed thiol groups of hexanethiol and hexanedithiol molecules. Cursor measurements of the nanoparticles revealed sizes ranged from 3 to 5 nm in diameter, and patterns were formed with a single layer of nanoparticles. The slower adsorption of the nanoparticles on shaved areas of the substrate compared to nanografting of molecular patterns was attributable to differences in mobility and concentration.

5.5.1 Electroless Deposition of Metals on Nanografted SAM Patterns

Site specific reactions for electroless deposition of metals were accomplished using nanografting. Copper nanostructures formed selectively on carboxylic acid terminated SAM patterns that were nanografted within a hydroxyl-terminated resist monolayer, using electroless plating without a catalyst [26]. To accomplish in situ studies, the AFM cantilevers were coated with silane to prevent copper deposition on the probe. An example showing selective growth of copper nanostructures on nanografted patterns of 16-mercaptohexadecanoic acid (16-MHA) is displayed in Fig. 5.5. A computer script was designed to automate the nanografting process to generate patterns of different line densities within a matrix SAM of 11-mercaptoundecanol (11-MUD), which resists copper deposition. The parameters of the tip trajectory during nanografting can be used to define the thickness of copper according to the density of grafted molecules. Lower density of carboxylic acid groups resulted in differences along the gradients for deposition of copper. Changes in the surface density of 16-MHA were systematically varied by designing the probe trajectory to advance either at the edges or centers of the patterns. The difference in the molecular gradients of 16-MHA nanopatterns was evaluated by introducing

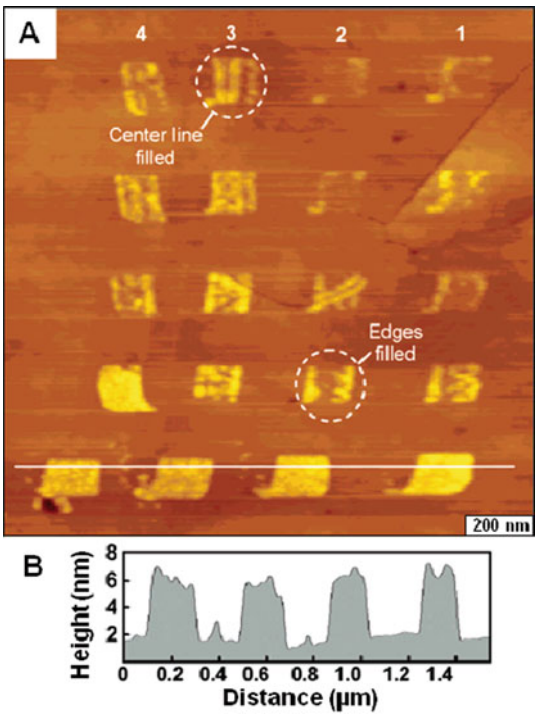

Fig. 5.5 Nanografted patterns of carboxylic acid terminated SAMs were generated with different densities for electroless deposition of copper. (**a**) View of copper nanopatterns grown on nanografted patterns written with different line densities; (**b**) cursor plot for copper structures of the bottom row. (Reprinted with permission from Ref. [26]. Copyright © American Chemical Society)

a copper solution. Metal ions (Cu^{2+}) deposited selectively in the reduced form as Cu^0 via an autocatalytic reaction on regions patterned with 16-MHA. For patterns written with lower density, less copper was observed to deposit. When the probe was traced only once (top rows) less copper deposition occurred compared to the bottom rows where the tip was swept twice along a linescan.

Systematically engineering the writing parameters for arrays of nanopatterns generated by automated nanografting offers a further useful strategy for controlling reaction conditions for bottom-up surface assembly. Essentially, the surface density of reactive moieties can be defined to further control spatial parameters of surface reactions. In addition, the writing path itself was shown to influence the initial stages of metal deposition. The general approach for patterning metals with electroless deposition could readily be extended to other metals such as platinum or nickel for construction of a range of metal structures and nanoscale metal junctions.

5.6 Nanografting with Porphyrins

An obstacle for producing patterns with nanografting has been the limitation of using thiol-based chemistries. New directions are being developed for expanding beyond preliminary model systems of chemisorbed *n*-alkanethiols on gold substrates to other chemical linkers. Porphyrins and metalloporphyrins have a

macrocyclic tetrapyrrole structure, which may be functionalized with various substituents. The choice of focusing research efforts on model systems of porphyrins is highly practical, because of the associated electrical, optical and chemical properties of this functional class of molecules. More complex surface structures could be achieved with nanografting by using porphryins with thiolated substituents [35] or pyridyl functional groups [28]. Modifications of the macrocycle, peripheral groups or bound metal ions can generate a range of electrical, photoemissive or magnetic properties. The orientation of porphyrins on surfaces is determined by factors such as the nature of the peripheral substituents and their position on the macrocycle. The resulting surface structures influence the photonic and electronic properties of the systems. Also, different properties result when different metals are coordinated to the macrocycle. Porphyrin and metalloporphyrin systems are excellent materials for surface studies, due to their diverse structural motifs and associated electrical, optical and chemical properties, and thermal stability [63, 64]. The rigid planar structures and π-conjugated backbone of porphyrins convey robust electrical properties for potential molecular electronic devices.

Scanning probe studies of nanografted patterns of dipyridyl porphyrins were used to provide insight for the molecular orientation and surface assembly of porphyrins from mixed solvent media, with studies by LeJeune, et al., [65]. In situ AFM furnished local views of the assembly of porphryins with pyridyl-substituents on surfaces of Au(111). Experiments were accomplished for nanografting *n*-alkanethiols within a matrix film of 5,10-diphenyl-15,20-di-pyridin-4-yl-porphyrin (DPP) as well as for nanografting patterns of DPP within different matrix SAMs of *n*-alkanethiols. The solubility of porphyrins in ethanol, butanol or water are problematic for accomplishing in situ AFM studies, therefore a solvent mixture was used for nanografting. First the porphyrin was dissolved in a parent solution of dichloromethane, and then further diluted 100-fold in ethanol. Examples of nanografted porphyrin patterns are displayed in Fig. 5.6. Dodecanethiol (C12) was used as a matrix SAM for writing nanostructures of DPP in a solution containing 1% dichloromethane in ethanol. The overall final concentration of DPP used for nanografting was 1 micromolar.

A mosaic design of 20 oval patterns was produced by nanografting DPP within a C12 SAM, as shown in the AFM topograph of Fig. 5.6a. The patterns were produced by tracing the probe in a circular trajectory four times, so that the centers of the rings were not disturbed. The patterns were produced within 5 min using a scan speed of 0.1 μm/s. The dimensions of the oval structures of DPP measure 77 ± 3 nm from side to side, and 99 ± 6 nm from top to bottom. The dodecanethiol islands in the middle of the rings that are surrounded by a ring of DPP have an average diameter of 58 ±10 nm and furnish a convenient height reference for evaluating the depth of the DPP patterns. The distance between patterns ranged between 53 and 115 nm in the vertical direction and between 44 and 200 nm horizontally. A force of 2.3 nN was applied to write patterns of porphyrins within dodecanethiol while imaging in liquid media of mixed solvents. Characteristics of the underlying Au(111) substrate such as etch pits and scar defects are apparent in the 700 × 700 nm^2 topograph, indicating that after nanografting multiple patterns the probe still maintains a sharp

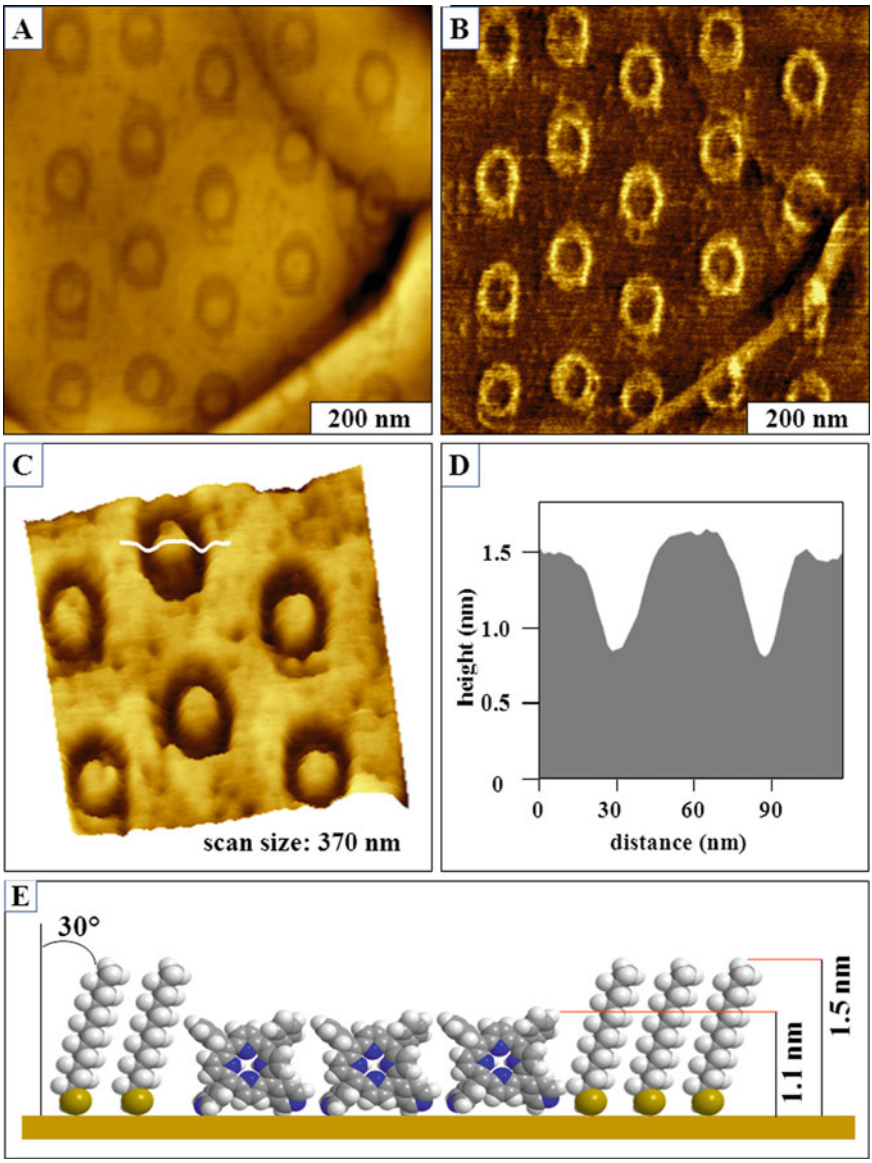

Fig. 5.6 Nanopatterns of diphenyl-dipyridyl porphyrin nanografted within dodecanethiol. (**a**) Mosaic design of 20 ring nanostructures viewed by an AFM topograph; (**b**) simultaneously acquired lateral force image; (**c**) magnified view; (**d**) cursor profile across one of the patterns traced in (**c**); (**e**) height model

geometry for accomplishing high-resolution imaging. The lateral force image (Fig. 5.6b) exhibits distinct contrast because of the different head groups of the C12 matrix and DPP nanopatterns. A zoom-in view of six ring nanopatterns is presented in Fig. 5.6c showing the fine details of the pattern shapes and height differences. The difference in height for the matrix dodecanethiol and DPP measures 0.5 ± 0.2 nm as shown by a representative line profile in Fig. 5.6d. This height difference corresponds to an upright configuration of DPP for a perpendicular orientation on Au(111) as shown by the molecular model of Fig. 5.6e.

For nanografted patterns of DPP, the heights measured from cursor profiles indicate that molecules assemble with an upright configuration with the porphyrin macrocycle oriented perpendicular to the substrate. As previously shown for nanografted molecules of *n*-alkanethiols which have a rod-like shape, planar macrocycles of DPP likewise are confined during nanografting. Constrained conditions prevent molecules of DPP from adopting a coplanar orientation on the surface to directly generate an upright configuration. The mechanical process of nanografting alters the assembly pathway providing a means to control molecular orientation of nanopatterned porphyrins on surfaces.

5.7 Nanografted Patterns of Proteins

Methods for nanoscale fabrication are becoming important for biochemical investigations, supplying tools for basic research concerning protein-protein interactions and protein function. Protein patterning is essential for the integration of biological molecules into miniature bioelectronic and sensing devices. Often, fabrication of functional nanodevices for biochemical assays requires that biomolecules be attached to surfaces with retention of structure and function. Nanoscale studies can facilitate the development of new and better approaches for immobilization and bioconjugation chemistries, which are key technologies in manufacturing surface platforms for biosensors. Nanografting provides a way to spatially control the deposition of proteins on well-defined, local areas of patterned surfaces for accomplishing in situ studies of biochemical reactions. The ability to define the chemical functionalities of nanografted patterns at nanometer length scales offers new possibilities for studies of biochemical reactions in controlled environments. Capturing AFM images in situ throughout the progressive steps of nanografting and surface patterning can disclose reaction details at a molecular level, providing direct visualization of biochemical reactions.

An overview of the different proteins that have been patterned with nanografting is summarized in Table 5.2, with spatial dimensions reaching the level of single molecule detection with protein monolayers. Spatially well-defined regions of surfaces can be nanografted with reactive or adhesive terminal groups for the attachment of biomolecules. The dimensions of many proteins are on the order of tens to hundreds of nanometers, therefore nanografting provides a way to generate patterns with appropriate sizes for defining the placement of individual proteins on surfaces. The terminal moieties of SAMs mediate the nature of protein binding,

Table 5.2 Protein studies accomplished in situ with nanografted patterns of SAMs

Biomolecule	Nanografted molecule	Pattern dimensions	Matrix SAM	Liquid media	Binding motifs	References
Antibiotin IgG	1-hexanethiol	5.2 nm × 5.2 nm	Thiolated biotin SAMs	Ethanol	Specific biotinylation	[32]
Gal	Thiolated Gal	130 nm × 110 nm	Octanethiol	Ethanol	S-Au carbohydrate ligand	[25]
GalCer	Thiolated GalCer	150 nm × 150 nm	1-decanethiol	Ethanol	S-Au carbohydrate ligand	[25]
De novo 4-helix bundle protein S-824-C	S-824-C protein	100 nm × 100 nm 200 nm × 200 nm	Octadecanethiol	Mixed aqueous buffer	S-Au single cysteine thiol	[37]
De novo maltose binding protein (MBP)	MBP	50 nm × 100 nm 100 nm × 200 nm	Undecanethiol triethylene glycol	Mixed aqueous buffer	S-Au double cysteine residues at C terminus	[36]
Lysozyme	$HS(CH_2)_2COOH$	10 nm × 150 nm 100 nm × 150 nm	Decanethiol	2-butanol	Electrostatic	[25]
Staphylococcal protein A (SpA)	Mercapto-hexadecanoic acid	100 nm × 100 nm	Octadecanethiol	Ethanol water EDC/NHS	Covalent activation chemistry	[29]
Bovine carbonic anhydrase	3-mercapto-1-propanoic acid 6-mercaptohexanol	400 nm × 400 nm	$C_{11}(EG)_6$	Water	Electrostatic	[73]
Rabbit IgG	11-mercapto-undecanoic acid	5,000 nm × 5,000 nm	Octanethiol	Buffer	Covalent	[74]

Table 5.2 (continued)

Biomolecule	Nanografted molecule	Pattern dimensions	Matrix SAM	Liquid media	Binding motifs	References
Bovine serum albumin	3-mercapto-1-propanal	200 nm × 250 nm	Hexanethiol	Buffer	Covalent	[30]
Rabbit IgG mouse anti-rabbit IgG	11-mercapto-undecanal	300 nm × 300 nm	Octadecanethiol	Buffer	Covalent	[24]
Acetylcholine esterase (AChE)	$HS(CH_2)_{11}$-$(OCH_2CH_2)_3OH$	~150 nm × 150 nm	$HS(CH_2)_{11}$ $(OCH_2CH_2)_6$ $O(CH_2)_{11}$-$CH(OH)CH_2OH$	Ethanol	Covalent	[87]
Insulin	$HS(CH_2)_{11}$-$(OCH_2CH_2)_3OH$	~150 nm × 150 nm	$HS(CH_2)_{11}$ $(OCH_2CH_2)_6$ $O(CH_2)_{11}$-$CH(OH)CH_2OH$	Ethanol	Covalent	[87]
Anti-mouse IgG	Mouse IgG	400 nm × 4,000 nm	Octadecanethiol	Ethanol	Antigen-antibody recognition	[88]
Three-helix bundle metalloproteins	C-terminal thiolated protein	NA	Octadecanethiol	Trifluoro-ethanol	S-Au	[36]
Maltose binding protein (MBP)	MBP with a double cysteine	NA	Undecanethiol triethylene glycol	Buffer	S-Au double cysteine thiol	[89]

such as through electrostatic interactions, covalent binding, molecular recognition or through specific interactions such as streptavidin-biotin recognition. The chemistry of SAM surfaces can be engineered to avoid non-specific protein adsorption for surrounding matrix monolayers, yet make specific interactions with selected proteins to be immobilized on nanografted patterns. Very few surfaces resist protein adsorption, and efforts have been directed to understand the mechanisms that contribute to protein resistance or adhesion to surfaces. Systematic studies of functionalized SAMs have been reported which evaluated the molecular characteristics that impart resistance to protein adsorption [66–71]. Depending on the protein of interest and buffer conditions, methyl-, hydroxyl- or glycol-terminated SAMs have been used effectively as matrices that resist non-specific protein adsorption.

The typical general steps of an in situ protein binding experiment with nanografting are to first graft nanopatterns of protein-adhesive *n*-alkanethiols within a resistive matrix, then rinse the liquid cell and inject a solution of proteins to bind to the SAM nanopatterns. In a final step, the activity of the immobilized proteins can be tested by introducing an antibody or protein which binds specifically to the surface-bound protein. With nanografting the same tips that are used to produce patterns are also used to characterize the morphology of nanopatterns after successive steps of protein adsorption. Unlike electron microscopy methods which require high vacuum chambers and conductive coatings for specimens, in situ AFM experiments can be accomplished under near-physiological conditions in aqueous buffered environments. With in situ nanografting, the protein patterns are not exposed to air or dried, and remain in a carefully controlled liquid environment by rinsing and exchanging solutions within the liquid cell. Sequential real time AFM images can disclose reaction details at a molecular level, revealing information about the adsorption kinetics and configurations of protein binding.

The first studies using nanografting to immobilize proteins were conducted in 1999 by Wadu-Mesthrige, et al., using protocols with either electrostatic or covalent interactions to immobilize lysozyme, rabbit immunoglobulin G (IgG) and bovine serum albumin (BSA) on SAM nanopatterns [31]. In these initial investigations, functionalized alkanethiol SAMs of carboxylic acid head groups or aldehydes were nanografted to mediate either electrostatic or covalent binding of IgG and lysozyme. Proteins were sustained on patterns despite steps of washing with buffer and surfactant solutions and were stable for at least 40 h of AFM imaging. The smallest protein feature yet produced by nanografting is a $10 \times 150\ nm^2$ line pattern containing three proteins [31].

5.7.1 Studies with Antigen-Antibody Binding Accomplished with Nanografting

The first successful AFM experiment reported that applied nanografting to study antigen-antibody binding in situ was conducted by Wadu-Mesthrige, et al., [30]. The activity of rabbit IgG immobilized covalently on an aldehyde-terminated pattern produced by nanografting was tested for reactivity toward monoclonal mouse anti-rabbit IgG. Six aldehyde-terminated nanopatterns of different sizes and arrangement

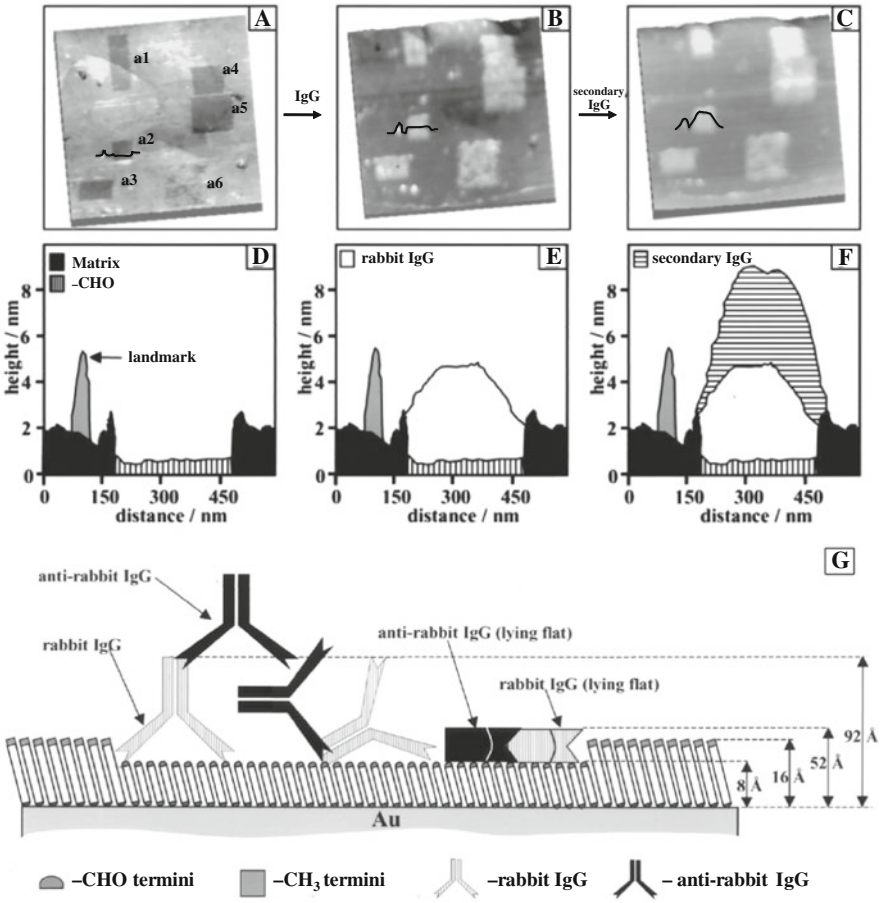

Fig. 5.7 The steps of protein binding and molecular recognition with nanografted patterns captured by AFM topographic images. (**a**) Six nanopatterns of 3-mercapto-1-propanal were written in a dodecanethiol SAM. (**b**) The image contrast changed after rabbit IgG bound covalently to the aldehyde-terminated nanopatterns. (**c**) After introducing mouse anti-rabbit IgG, the patterns display further height changes, indicating the antibody binds specifically to the protein nanopatterns. Cursor traces across pattern a2 indicate the height changes (**d**) after nanografting; (**e**) after injecting IgG; (**f**) after introducing anti-rabbit IgG. (**g**) Map for understanding the evolution of molecular height changes during the steps of this in situ experiment. (Reprinted with permission from Ref. [30])

were first grafted within a dodecanethiol SAM matrix (Fig. 5.7a). After injecting rabbit IgG and rinsing with a surfactant solution, selective adsorption of IgG was observed on all six nanopatterns (Fig. 5.7b). In the next step, mouse anti-rabbit IgG was introduced (Fig. 5.7c) revealing further increases in the heights of patterns. The changes in the height of nanopatterns before and after secondary IgG binding could be monitored in situ (cursor profiles, Fig. 5.7d–f), exhibiting thicknesses which correspond to the different surface configurations of IgG (Fig. 5.7g). Changes in pattern

heights were used to assess whether the immobilization chemistry resulted in a side-on or an end-on orientation for IgG molecules. The reactivity and stability of protein nanopatterns was studied in further reports, with investigations of the retention of specific activity of the immobilized proteins for binding antibodies [24, 30].

5.7.2 Protein Binding on Activated SAM Patterns

Chemical activation of carboxylic acid terminated SAMs was accomplished for nanografted patterns of staphylococcal protein A (SpA) through covalent linkage by Ngunjiri, et al., [29]. The carboxylic acid head groups of SAMs were activated using 1-ethyl-3-(3-dimethylaminopropyl) carbodiimide hydrochloride (EDC) and N-hydroxysuccinimide (NHS) coupling chemistries [72]. The activation of carboxylic acid groups of nanografted patterns of 11-mercaptoundecanoic acid (11-MUA) was accomplished by immersing the substrate in an aqueous 1:1 mixture of NHS/EDC for 30 min to generate an activated complex with a stable reactive intermediate (N-succinimidyl ester). The resulting NHS ester interacts by a nucleophilic substitution reaction with accessible α-amine groups present on the N-termini of proteins or with ε-amines on lysine residues. The proteins bind covalently to nanografted patterns by forming a Schiff's base linkage to make complexes with the carboxylic acid groups of 11-MUA. For the in situ protein patterning experiment with SpA, 16 square nanopatterns (100×100 nm^2) of 11-MUA were written within a matrix octadecanethiol (ODT) SAM arranged in a 4×4 array (Fig. 5.8a–c). The nanopatterns were spaced 50 nm apart within each row, and the rows were spaced at 100 nm intervals. After nanografting, a 1:1 aqueous solution of 0.2 M EDC and 0.05 M NHS was introduced into the AFM cell to react for 30 min. The cell was then rinsed twice with phosphate-buffered saline, and a solution of 0.05 mg/mL SpA solution was introduced and incubated for 30 min. Finally, the cell was rinsed with water and ethanol to completely remove any unreacted protein. After chemical activation and protein immobilization, the same array of nanostructures was imaged in ethanol with AFM (Fig. 5.8d–f). All of the steps of nanografting, NHS/EDC activation of carboxylate groups, and protein adsorption were accomplished in situ with the same tip, and the entire experiment was completed in ~3 h. The SpA molecules were shown to bind selectively to the 11-MUA nanopatterns, forming a single layer of protein attached to nanopatterns of 11-MUA.

For in situ studies of biochemical reactions using nanografting, the most suitable immobilization chemistries for nanoscale experiments should proceed under aqueous conditions to preserve protein activity. Also, investigations should be completed using very dilute protein and reagent solutions to slow the reaction rate so that the reaction transpires over time intervals of 20–30 min. A potential technical detail is that the motion and force of the scanning tip can sweep away adsorbates or perturb the reaction environment. To address this concern, the immobilization chemistry selected for patterning must be sufficiently robust to enable continuous imaging and scanning by the tip. Imaging in liquids enables using small imaging

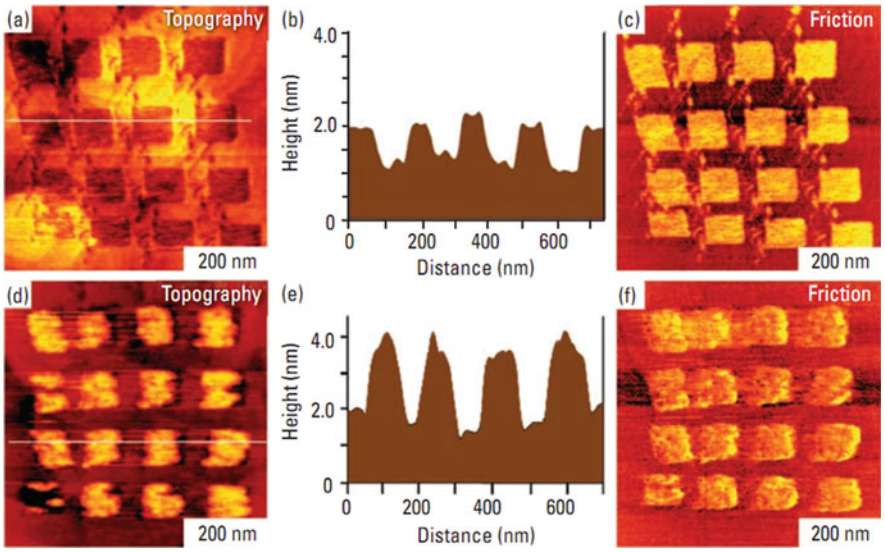

Fig. 5.8 Nanoscale protein assay of the adsorption of SpA on nanografted patterns. (**a**) An array of 11-MUA squares written in an ODT matrix SAM, (**b**) cursor plot along the white line; (**c**) corresponding lateral force image for (**a**); (**d**) same area after EDC/NHS activation and subsequent adsorption of SpA; (**e**) cursor plot along the white line in (**d**); (**f**) simultaneously acquired lateral force image for (**d**). (Reprinted with permission from Ref. [29], Copyright © American Chemical Society)

forces (0.005–0.2 nN) because the adhesive interactions between the tip and sample are minimized. An intrinsic advantage for these protocols is that small forces in the range of piconewtons to nanonewtons can be precisely controlled with AFM instruments.

5.7.3 In Situ Studies of Protein Adsorption on Nanografted Patterns

Nanografting has been applied by several investigators to write nanopatterns for studies of protein immobilization and reactivity. Zhou et al. evaluated protein adsorption at the nanoscale by comparing differently functionalized SAMs side-by-side using nanografting [3, 73]. Protein adsorption on three differently charged linkers nanografted within a hexa(ethylene glycol) terminated alkanethiol resist SAM, was monitored in situ by AFM at different pH conditions. The adsorption of proteins onto nanografted patches of 6-mercaptohexan-1-ol (MCH), *n*-(6-mercapto hexyl) pyridinium bromide (MHP), and 3-mercaptopropionic acid (MPA), was studied with lysozyme, IgG and carbonic anhydrase II. They concluded that the overall charge of protein molecules as well as the charge of local domains of the proteins plays a role in immobilization. In the same report, nanografting was applied to

assemble multilayered protein G/IgG/anti-IgG nanostructures through electrostatic interactions, as an approach to orient IgG molecules for antibody-based biosensor surfaces.

Using SPL methods of nanografting and nanoshaving, Kenseth, et al. compared three approaches for protein patterning [74]. Nanografting was successfully combined with immobilization of IgG through EDC activation of 11-MUA acid and also through chemisorption of a disulfide coupling agent, dithiobis(succinimidyl undecanoate). Insulin and acetylcholinase esterase were immobilized on nanografted 1,2-diols which were activated by sodium periodate to produce aldehyde groups, reported by Jang, et al., [75]. Retention of catalytic activity was demonstrated for nanografted patterns of enzymes.

5.7.4 Direct Nanografting of Proteins Modified with Thiol Residues

Nanografting was applied to directly pattern designed metalloproteins by Au-S chemisorption by Case, et al., [36]. A 3-helix bundle protein structure with a 78 amino acid iron(II) complex was nanografted into an ethylene glycol-terminated SAM. The protein was designed to present the C-termini of three helices, terminated with D-cysteine residues for attachment to gold surfaces. The heights of nanografted patterns of this protein measured 5.3 nm, in good agreement with the dimensions predicted theoretically for the *de novo* protein to assemble in a upright orientation normal to the Au(111) substrate. A *de novo* 4-helix bundle protein was nanografted within an ODT matrix through a single cysteine thiol by Hu, et al., [37]. The protein used for these studies was engineered to have a glycine-glycine-cysteine tag at its C-terminus for attachment to the gold surface through a single cysteine thiol.

Maltose Binding Protein (MBP) was successfully patterned using nanografting by Staii, et al., [76]. The MBP protein was engineered to terminate with a double-cysteine residue for chemisorptive binding to gold surfaces. The biochemical activity of the substrate immobilized proteins was verified in situ, demonstrating that MBP function is not altered by either the immobilization process, the spatial confinement associated with the surrounding proteins, or protein-substrate interactions. The dependence of the frictional force upon the maltose concentration was used to extract the dissociation constant: $k_d = 1 \pm 0.04$ μM for this system, detecting maltose at the level of tens of attograms.

5.7.5 Reversal Nanografting

An approach for "reversal" nanografting was introduced for regulating surface heterogeneity to control protein binding [32]. As with nanografting, the reversal method also has three main steps of imaging, shaving-and-replacement, and

imaging again. However, rather than directly nanografting desired termini for protein binding, the matrix SAMs are made of the binding termini, and nanografted thiols are used to isolate and separate well- defined areas of the matrix SAMs to generate ultra-small domains of protein binding sites. By controlling the shaving size and the spacing between the shaving lines, broad areas of arrays of regular nanostructures were rapidly fabricated, achieving dimensions of 5–30 nm for nanografted patterns. Reversal nanografting was demonstrated with an array of thiolated biotin nanostructures which were reacted with antibiotin IgG. Within a single experiment, reversal nanografting produced 1,089 biotin nanostructures measuring with 5.2 nm × 5.2 nm; 288 nanostructures with dimension of 12.7 nm × 12.7 nm; and 144 nanopatterns with dimensions of 10.3 nm × 31.9 nm. Thus, by changing the dimension and separation of each element of nanografted arrays the coverage and orientation of protein molecules can be regulated at the molecular level.

Although not yet practical for high throughput applications and manufacturing, combining the in situ steps of nanografting with protein immobilization enables new approaches for directly investigating changes that occur on surfaces during biochemical reactions from the bottom-up. In situ AFM investigations of protein reactions are valuable for studying antigen-antibody binding at the nanometer scale, for assessing the specificity of protein-protein binding, and for evaluating the orientation of immobilized proteins and the corresponding accessibility of ligands for binding.

5.8 Patterns of DNA Produced by Nanografting

Surface platforms of arrays of DNA patterns are used for studies with gene mapping, drug discovery, DNA sequencing and disease diagnosis. Scanning probe-based experiments offer compelling advantages and opportunities for high sensitivity, label-free detection with studies of molecular-level phenomena. Initial studies have been advanced using nanografting to prepare patterns of DNA with successive steps of enzyme digestion [33, 77], hybridization studies [78–80], as well as DNA-mediated binding of proteins [81]. A comparison of the different DNA systems and pattern dimensions produced by nanografting is provided in Table 5.3.

Individual DNA molecules can be localized within mixed patterns by diluting DNA with another alkanethiol molecule. To achieve single-molecule precision, Josephs et al., nanografted thiolated double-stranded DNA (dsDNA) with 94 base pairs from a solution containing a ~10000:1 mixture of aminoundecanethiol and dsDNA [82]. By diluting DNA molecules with another alkanethiol molecule, DNA can be positioned on a chemically well-defined, atomically flat surface and be imaged in situ. One to four dsDNA molecules were localized confined within a nanografted area to provide high precision for positioning individual DNA molecules within biochemical structures.

Table 5.3 Studies reported with nanografted patterns of DNA

System	Pattern sizes	Matrix film	Liquid media	Year	References
DNA-derivatized gold nanoparticles	100 nm × 50 μm lines	Octadecanethiol	Buffer: 1 M NaCl, 10 mM phosphate, pH 7	2001	[79]
Single stranded DNA (ssDNA) 5′-HS $(CH_2)_6$-CTAGCTCTAATCTGCTAG 5′-HS $(CH_2)_6$-AGAAGGCCTAGA	Dimensions in nm: 115 × 135; 190 × 255; 20 × 170; 15 × 150; 25 × 160	1-hexanethiol 1-decanethiol	Mixed solvent of 2-butanol/ water/ ethanol 6:1:1 (v/v/v) containing 40 μM ssDNA.	2002	[33]
Single stranded DNA 5′-HS-$(CH_2)_6(T)_{15}$ 3′-HS-$(CH_2)_6(T)_{25}$ 5′-HS-$(CH_2)_6(T)_{35}$ 5′-HS$(CH_2)_6$ ACTGCACATGGCGTG TTGCGGTGATT CGCGTTGGT	Dimensions in nm: 120 × 200; 100 × 380; 100 × 200; 250 × 250; 80 × 220; 100 × 400; 180 × 250; 40 × 250; 150 × 75	1-decanethiol	Mixed solvent of water saturated with 2-butanol and ethanol (6:1)	2005	[78]
Nanografted patterns of mercaptoethanol were used to evaluate thickness of DNA SAMs	300 × 300 nm squares of 2-mercaptoethanol	HSC_6H_{12}-5′-CCCT AACCCTAACCCTAA CCC-3′-rhodamine green 5′-GTGTTAGGT TTAGGGTTAGTG-3′	Phosphate buffered saline (pH 4.5)	2006	[50]
λ-DNA adsorbed to octadecyldimethyl-monochloro-silane (C18DMS)	100 nm × 3 μm lines of (C18DMS)	Octadecyldimethyl monochlorosilane	Nanografted patterns were incubated with λ-DNA in TE buffer (pH 7.2)	2007	[83]
Thiolated ssDNA	300 nm × 300 nm to 1 μm × 1 μm	Oligo-ethyleneglycol modified thiols	1:1 mixture of buffer and ethanol	2008	[80]

Table 5.3 (continued)

System	Pattern sizes	Matrix film	Liquid media	Year	References
ssDNA with 44 base pairs	1 μm × 1 μm	Top-oligo ethylene-glycol (EG) HS-$(CH_2)11$-$(EG)_3$-OH	Thiol-DNA containing 3:2 mixtures (v/v) of 1 M buffer and ethanol	2008	[77]
ssDNA-mediated binding of proteins thiol modified oligonucleotides	200 nm × 200 nm to 1 μm × 1 μm	Ethylene glycol- terminated alkylthiols	1:1 mixture of buffer and ethanol	2009	[81]
94 basepair thiolated double stranded DNA attached to nanografted patterns	50 nm × 50 nm	Octadecanethiol	Mixture of 11-aminoundecane thiol with DNA (10,000:1) in Tris acetate EDTA (TAE)	2010	[82]
Thiol derivatized single-stranded oligonucleotide HS-C_6H_{12}-5′-AGA TCA GTG CGT CTG TAC TAG CAC A-3′ and complementary sequence	0.5–1 μm	6-mercapto-1-hexanol	10 μM probe DNA in a 1:1 mixture (v/v) of STE-buffer and absolute ethanol	2010	[90]

5.8.1 *In Situ Studies of Hybridization with Nanografted Patterns of ssDNA*

Nanostructures of single stranded oligonucleotides or single stranded DNA (ssDNA) have been produced with nanografting for molecular-level studies of DNA hybridization [77–80]. Label-free hybridization of ssDNA nanostructures was accomplished for nanografted patterns of ssDNA incubated with complementary segments of designed sequences [78]. To mediate attachment to gold surfaces for nanografting, the DNA molecules were designed to contain a short thiol linker at either the 3′ or 5′ end. These investigations provide information about the specificity, kinetics and selectivity of surface-bound ssDNA for hybridization with complementary strands.

Label-free hybridization of nanostructures has proven to be highly selective and sensitive; as few as 50 molecules can be detected by in situ AFM studies [78]. The efficiency of the hybridization reaction at the nanometer scale depends sensitively on the packing density of DNA within the nanostructures [77, 78, 80]. The density of ssDNA molecules within nanografted patterns can be regulated by changing certain experimental parameters such as written line density and concentration. The structure of nanografted patterns and the relative surface orientation of the ssDNA molecules have been determined in situ using AFM to show that molecules of ssDNA adopt a standing upright orientation.

Nanopatterns of thiolated ssDNA were produced using nanografting by Maozi Liu, et al., [33]. Thiolated ssDNA molecules adsorb chemically onto exposed areas of gold through sulfur-gold chemisorption. The ssDNA molecules within nanopatterns adopt an upright, standing orientation on gold surfaces which were found to be accessible by enzymes. A ssDNA pattern (115×135 nm^2) of an 18-nucleotide oligomer (5′-HS-$(CH_2)_6$-CTAGCTCTAATCTGCTAG) was nanografted into a hexanethiol matrix, as shown in Fig. 5.9a. Nanografting and imaging of the patterns were conducted in a mixed solvent of 2-butanol/water/ethanol with a (v/v/v) ratio of 6:1:1 containing 40 μM ssDNA. The heights of the nanografted patterns were found to match well with the theoretical dimensions of an upright configuration of DNA, shown with cursor profiles. In Fig. 5.9c, a second 12-mer ssDNA (5′-HS-$(CH_2)_6$-AGAAGGCCTAGA) was grafted into a dodecanethiol SAM. Line patterns of ssDNA as narrow as 10 nm were produced, as shown in Fig. 5.9e. Three lines of the 12-nucleotide oligomer were nanografted within decanethiol.

Unlike natural, unconfined solution adsorption of thiolated DNA on gold surfaces, in which DNA oligomers tend to assemble with the backbone parallel to the substrate in a lying down configuration, nanografted patterns of ssDNA form a standing conformation, confined by the surrounding matrix monolayer to generate a fairly dense, close-packed structure of upright strands [33, 78]. The alkanethiol matrix SAM guides the adsorption of DNA to define the geometry and packing of grafted ssDNA molecules. Upright ssDNA molecules within the nanografted structures maintain their reactivity, as demonstrated by hybridization reactions with complementary DNA in solution. The hybridization and corresponding control experiments indicate that nanografted patterns of ssDNA exhibit high specificity and selectivity towards complementary strands.

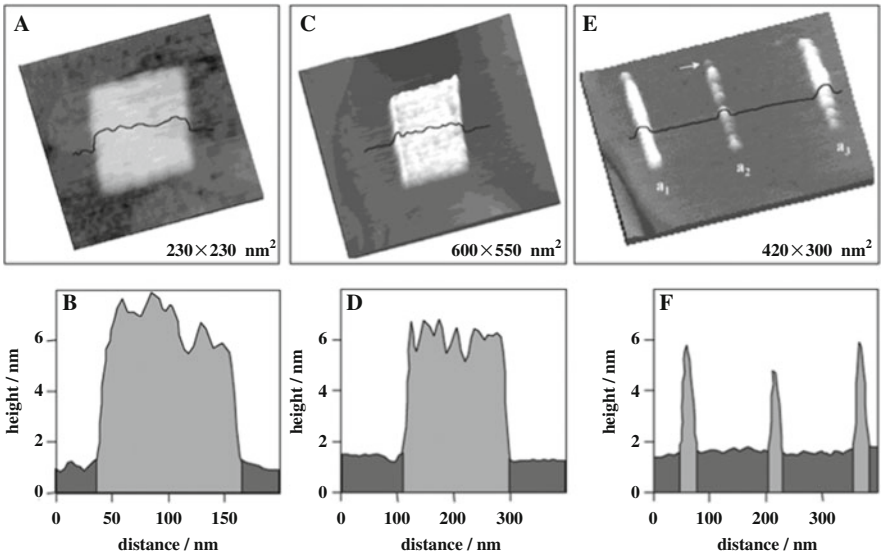

Fig. 5.9 Patterns of single-stranded DNA were nanografted into an alkanethiol SAM matrix. (**a**) Topograph of an 18-nucleotide ssDNA nanografted into a hexanethiol SAM (115 × 135 nm^2); (**b**) corresponding profile for the line in (**a**). (**c**) Nanografted rectangle (190 × 255 nm^2) of ssDNA with 12 nucleotides inscribed within a dodecanethiol matrix; (**d**) cursor profile for (**c**). (**e**) Line patterns of the ssDNA 12-mer nanografted into decanethiol; (**f**) profile for (**e**). The 18-mer and 12-mer ssDNA strands are 5′-HS-$(CH_2)_6$-CTAGCTCTAATCTGCTAG and 5′-HS-$(CH_2)_6$-AGAAGGCCTAGA, respectively. (Reproduced with permission from reference [33], Copyright © American Chemical Society)

5.8.2 *Reactions with Restriction Enzymes Studied Using Nanografted Patterns of DNA*

Time-dependent AFM images were acquired in situ for a nanografted pattern of the 18-nucleotide oligomer during digestion by the enzyme shown in Fig. 5.9a. The RQ1 DNase I enzyme endonucleotically degrades DNA to produce oligonucleotide fragments at the 3′ end with a hydroxyl terminal group. After nanografting steps, the ssDNA patterns were rinsed and the solvent was then replaced sequentially by ethanol, water, and finally buffer solution. Next, RQ1 DNase I was introduced and surface changes were captured in situ with high-resolution AFM images. The liquid cell experiment establishes that upright, densely-packed strands of DNA within nanografted patterns are accessible to enzyme digestion.

Studies with the cutting action of restriction enzymes were accomplished by Castronovo, et al. to better understand enzyme/DNA interactions [77]. An enzymatic reaction (*DpnII* restriction digestion) with DNA nanopatterns of variable density (surface coverage) was investigated to understand the effect of molecular crowding on the accessibility of the DNA molecules to the restriction enzyme. Single-stranded DNA molecules containing 44 base pairs (bps) with a 4 base pair recognition sequence (specific to the *DpnII* restriction enzyme) in the middle

were patterned by nanografting. The resulting nanostructures were then hybridized with a complementary ssDNA sequence of the same length to yield patterns of restriction-ready double stranded DNA. The surface density of the DNA nanostructures produced by nanografting can be tuned by changing the writing parameters or by changing the concentration of the DNA when grafting. The study demonstrates that the *DpnII* restriction enzyme is sensitive to the DNA packing density; the enzymatic reaction is inhibited when the DNA density is higher than a certain threshold density within nanografted patterns.

5.8.3 Binding of Proteins to Nanografted Patterns of DNA

Hybrid nanostructures of DNA-protein conjugates can be produced for nanografted patterns of DNA oligomers with site-specific DNA-directed immobilization of proteins, as reported by Bano, et al., [81]. In the first step, nanografted patches of thiolated ssDNA were generated within a monolayer of ethylene glycol-terminated alkylthiols ($HS\text{-}(CH_2)_{11}\text{-}(OCH_2CH_2)_3\text{-}OH$) on Au(111) substrates. In subsequent reaction steps, proteins covalently modified with cDNA sequences were immobilized onto the $1 \times 1\ \mu m^2$ nanografted patterns. A covalent conjugate of streptavidin tethered with a DNA oligomer was found to bind to the nanografted ssDNA pattern by sequence-specific DNA hybridization. The surface was carefully rinsed with phosphate buffered saline to remove any physically adsorbed molecules and imaged with AFM between successive biochemical reaction steps. Changes in heights of the patterns enabled label-free detection of protein binding between each step of the reactions, which were likewise accomplished in multiplex experiments with control samples of streptavidin that did not have the complementary DNA tethers. The nanopatterns of DNA-protein conjugates were then used for further studies of selected protein-protein interactions with an anti-streptavidin immunoglobulin G as well as with the biomedically relevant matrix of human serum. The fabrication of nanografted arrays of multiple proteins in this study demonstrates that the interactions of biomolecular recognition mediated by DNA-protein recognition are highly specific and that bound proteins retain activity for further selective binding of proteins.

5.8.4 Using Nanografted SAM Patterns to Mediate Binding of DNA

Nanografted patterns of an aminopropyldiethoxysilane (APDES) SAM were used as sites for selective adsorption of DNA within matrices of octyldimethylmonochlorosilane (C8DMS) monolayers by Lee, et al., [83]. Line patterns of APDES that were 100 nm wide were nanografted in a C8DMS monolayer prepared on silicon dioxide substrates. After incubation in a 10 ng/μL solution of λ-DNA in buffer (pH 7.2) the heights of the nanopatterns was increased and revealed the shapes

of individual DNA strands. The negatively charged DNA deposited on the positively charged amine-functionalized line patterns of aminosilanes. The negatively charged DNA molecules bound to nanografted patterns via electrostatic interactions with the positively charged amine groups of APDES, but did not bind to matrix areas terminated with methyl headgroups. These investigations provide a fundamental step toward sensitive DNA detection and construction of complex DNA architectures on surfaces.

Nanografting provides a useful protocol towards sensitive DNA detection and likely attains the most sensitive detection levels yet achievable for label-free assays. The DNA nanopatterning methodology provides a unique opportunity for engineering biostructures with nanometer precision, which benefits the advancement of technologies for DNA biosensors and biochips.

5.9 Limitations of AFM-Based Nanografting

Thus far, the capabilities for molecular manipulation by nanografting have primarily been a tool for academic research. However one may anticipate that nanografting will eventually provide commercial value for chemical or biochemical sensing or for nanotechnology. A potential disadvantage for nanografting is that over time, molecular exchange reactions take place between solution molecules and the matrix SAM for certain systems of alkanethiol matrices. Natural processes of self-exchange become an issue specifically when nanografting longer chain alkanethiols into a shorter chain matrix layer, thus it is important to use dilute ($< 0.1\ \mu M$) solutions for nanografting. Depending on the nature and age of the matrix SAM, exchange reactions can be detected within 2–4 h when molecules from solution adsorb onto defect sites and at step edges. Software addresses this problem by enabling rapid automation of the nanofabrication process. Hundreds of exquisitely regular patterns can be produced within an hour or less, leaving sufficient time to progress to further in situ steps of reactions before exchange reactions have occurred.

The serial nature of nanografting with a single probe may be a problem for applications that require higher throughput, such as at scales of millions of nanostructures. Prototype arrays of 1,024 and 55,000 AFM probes have been developed for high-throughput nanopatterning [84, 85]. At this time, nanoscale studies with AFM enable new approaches to refine and optimize parameters used to link and organize proteins and other nanomaterials on surfaces. With in situ AFM characterizations, the orientation, reactivity, and stability of molecules adsorbed on SAM nanostructures can be monitored with successive time-lapse images using liquid AFM. These investigations provide the groundwork for advancing nanotechnology toward the nanoscale and furnish molecular-level information through the visualization of surface reactions.

5.10 Future Prospectus

Nanografting provides a practical tool to precisely control the arrangement of molecules on surfaces to enable bottom-up nanofabrication of structures through successive chemical reactions. In situ AFM studies with nanografting furnish opportunities for visualization, physical measurements and precise manipulation molecules at the nanometer scale. There are multiple advantages for nanografting, particularly because experiments are accomplished using liquid media. Advantages are the ability to precisely produce nanometer-sized patterns of metals, polymers, proteins and DNA with the benefits of successively imaging and accomplishing fabrication within well-controlled environments. Because so many chemical reactions can be accomplished in solution, there are rich possibilities for studying other surface reactions, in ambient, cooled or heated conditions. The capabilities for capturing real time images throughout sequential steps of reactions offer intriguing possibilities for new studies, with directly viewing the role of temperature, reagents and solvents. Nanografting protocols provide an additional unique capability for defining spatial parameters for controlling surface coverage and confining reactions within defined boundaries. The challenge for future research directions will be to achieve greater complexity for experiments for building ever more sophisticated 3D architectures from the bottom-up.

Acknowledgements The authors received financial support from the National Science Foundation (DMR-0906873) and also from the Dreyfus Foundation for a Camille Dreyfus Teacher-Scholar award. Wilson K. Serem is an LSU doctoral candidate supported by study-leave from Masinde Muliro University, Kenya, Africa.

References

1. A. B. Chwang, E. L. Granstrom, C. D. Frisbie, Fabrication of a sexithiophene semiconducting wire: Nanoshaving with an atomic force microscope tip, *Adv. Mater.* **12**, 285–288 (2000).
2. J. Shi, J. Chen, P. S. Cremer, Sub-100 nm patterning of supported bilayers by nanoshaving lithography, *J. Am. Chem. Soc.* **130**, 2718–2719 (2008).
3. D. Zhou, A. Bruckbauer, L. Ying, C. Abell, D. Klenerman, Building three-dimensional surface biological assemblies on the nanometer scale, *Nano Lett.* **3**, 1517–1520 (2003).
4. L. G. Rosa, J. Jiang, O. V. Lima, J. Xiao, E. Utreras, P. A. Dowben, L. Tan, Selective nanoshaving of self-assembled monolayers of 2-(4-pyridylethyl)triethoxysilane, *Mater. Lett.* **63**, 961–964 (2009).
5. J. E. Headrick, M. Armstrong, J. Cratty, S. Hammond, B. A. Sheriff, C. L. Berrie, Nanoscale patterning of alkyl monolayers on silicon using the atomic force microscope, *Langmuir* **21**, 4117–4122 (2005).
6. J. C. Garno, J. D. Batteas, in *Applied scanning probe methods, vol. IV, industrial applications,* B. Bhushan, Ed. (Springer, Berlin; Heidelberg; New York, 2006).
7. Z. M. LeJeune, W. Serem, A. T. Kelley, J. N. Ngunjiri, J. C. Garno, in *Encyclopedia of nanoscience and technology, (2nd edition),* H. S. Nalwa, Ed. (American Scientific Publishers, Stevenson Ranch, CA, 2010).
8. S. Xu, G. Y. Liu, Nanometer-scale fabrication by simultaneous nanoshaving and molecular self-assembly, *Langmuir* **13**, 127–129 (1997).

9. S. Xu, S. Miller, P. E. Laibinis, G. Y. Liu, Fabrication of nanometer scale patterns within self-assembled monolayers by nanografting, *Langmuir* **15**, 7244–7251 (1999).
10. D. S. Ginger, H. Zhang, C. A. Mirkin, The evolution of dip-pen nanolithography, *Angew. Chem. Int. Ed.* **43**, 30–45 (2004).
11. K. Salaita, Y. H. Wang, C. A. Mirkin, Applications of dip-pen nanolithography, *Nat. Nanotechnol.* **2**, 145–155 (2007).
12. A. T. Kelley, J. N. Ngunjiri, W. K. Serem, J.-J. Yu, S. Lawrence, S. Crowe, J. C. Garno, Applying AFM-based nanofabrication for measuring the thickness of nanopatterns: The role of headgroups in the vertical self-assembly of ω-functionalized *n*-alkanethiols, *Langmuir* **26**, 3040–3049 (2010).
13. C. A. Hacker, J. D. Batteas, J. C. Garno, M. Marquez, C. A. Richter, L. J. Richter, R. D. vanZee, C. D. Zangmeister, Structural and chemical characterization of monofluoro-substituted oligo(phenylene-ethynylene) thiolate self-assembled monolayers on gold, *Langmuir* **20**, 6195–6205 (2004).
14. N. A. Amro, S. Xu, G.-Y. Liu, Patterning surfaces using tip-directed displacement and self-assembly, *Langmuir* **16**, 3006–3009 (2000).
15. W. T. Muller, D. L. Klein, T. Lee, J. Clarke, P. L. McEuen, P. G. Schultz, A strategy for the chemical synthesis of nanostructures, *Science* **268**, 272–273 (1995).
16. J. J. Davis, C. B. Bagshaw, K. L. Busuttil, Y. Hanyu, K. S. Coleman, Spatially controlled Suzuki and Heck catalytic molecular coupling, *J. Am. Chem. Soc.* **128**, 14135–14141 (2006).
17. J. J. Davis, K. S. Coleman, K. L. Busuttil, C. B. Bagshaw, Spatially resolved Suzuki coupling reaction initiated and controlled using a catalytic AFM probe, *J. Am. Chem. Soc.* **127**, 13082–13083 (2005).
18. H. Lee, S. A. Kim, S. J. Ahn, H. Lee, Positive and negative patterning on a palmitic acid Languir–Blodgett monolayer on Si surface using bias-dependent atomic force microscopy lithography, *Appl. Phys. Lett.* **81**, 138–140 (2002).
19. J. Gu, C. M. Yam, S. Li, C. Cai, Nanometric protein arrays on protein-resistant monolayers on silicon surfaces, *J. Am. Chem. Soc.* **126**, 8098–8099 (2004).
20. H. G. Hansma, J. Vesenka, C. Siegerist, G. Kelderman, H. Morrett, R. l. Sinsheimer, V. Elings, C. Bustamante, P. K. Hansma, Reproducible imaging and dissection of plasmid DNA under liquid with the atomic force microscope, *Science* **256**, 1180–1184 (1992).
21. A. L. Weisenhorn, P. Maivald, H. J. Butt, P. K. Hansma, Measuring adhesion, attraction, and repulsion between surfaces in liquids with an atomic-force microscope, *Phys. Rev. B* **45**, 11226–11232 (1992).
22. J. N. Ngunjiri, A. T. Kelley, Z. M. LeJeune, J.-R. Li, B. Lewandowski, W. K. Serem, S. L. Daniels, K. L. Lusker, J. C. Garno, Achieving precision and reproducibility for writing patterns of n-alkanethiol SAMs with automated nanografting, *Scanning* **30**, 123–136 (2008).
23. S. Cruchon-Dupeyrat, S. Porthun, G. Y. Liu, Nanofabrication using computer-assisted design and automated vector-scanning probe lithography, *Appl. Surf. Sci.* **175**, 636–642 (2001).
24. G. Y. Liu, N. A. Amro, Positioning protein molecules on surfaces: A nanoengineering approach to supramolecular chemistry, *Proc. Natl. Acad. Sci. USA* **99**, 5165–5170 (2002).
25. M. Liu, N. A. Amro, G.-Y. Liu, Nanografting for surface physical chemistry, *Ann. Rev. Phys. Chem.* **59**, 367–386 (2008).
26. J. C. Garno, C. D. Zangmeister, J. D. Batteas, Directed electroless growth of metal nanostructures on patterned self-assembled monolayers, *Langmuir* **23**, 7874–7879 (2007).
27. J. C. Garno, Y. Y. Yang, N. A. Amro, S. Cruchon-Dupeyrat, S. W. Chen, G. Y. Liu, Precise positioning of nanoparticles on surfaces using scanning probe lithography, *Nano Lett.* **3**, 389–395 (2003).
28. Z. M. LeJeune, M. McKenzie, E. Hao, M. G. H. Vicente, B. Chen, J. C. Garno, Surface assembly of pyridyl-substituted porphyrins on Au(111) investigated in situ using scanning probe lithography, *SPIE Proceedings* **7593**, 759311 (2010).
29. J. N. Ngunjiri, J. C. Garno, AFM-based lithography for nanoscale protein assays, *Anal. Chem.* **80**, 1361–1369 (2008).

30. K. Wadu-Mesthrige, N. A. Amro, J. C. Garno, S. Xu, G. Y. Liu, Fabrication of nanometer-sized protein patterns using atomic force microscopy and selective immobilization, *Biophys. J.* **80**, 1891–1899 (2001).
31. K. Wadu-Mesthrige, S. Xu, N. A. Amro, G. Y. Liu, Fabrication and imaging of nanometer-sized protein patterns, *Langmuir* **15**, 8580–8583 (1999).
32. Y. H. Tan, M. Liu, B. Nolting, J. G. Go, J. Gervay-Hague, G. Y. Liu, A nanoengineering approach for investigation and regulation of protein immobilization, *ACS Nano* **2**, 2374–2384 (2008).
33. M. Liu, N. A. Amro, C. S. Chow, G.-Y. Liu, Production of nanostructures of DNA on surfaces, *Nano Lett.* **2**, 863–867 (2002).
34. S. M. D. Watson, K. S. Coleman, A. K. Chakraborty, A new route to the production and nanoscale patterning of highly smooth, ultrathin zirconium films, *ACS Nano* **2**, 643–650 (2008).
35. Y.-H. Chan, A. E. Schuckman, L. M. Perez, M. Vinodu, C. M. Drain, J. D. Batteas, Synthesis and characterization of a thiol-tethered tripyridyl porphyrin on Au(111), *J. Phys. Chem. C* **112**, 6110–6118 (2008).
36. M. A. Case, G. L. McLendon, Y. Hu, T. K. Vanderlick, G. Scoles, Using nanografting to achieve directed assembly of *de novo* designed metalloproteins on gold, *Nano Lett.* **3**, 425–429 (2003).
37. J. Hu, A. Das, M. H. Hecht, G. Scoles, Nanografting de novo proteins onto gold surfaces, *Langmuir* **21**, 9103–9109 (2005).
38. S. Xu, S. J. N. Cruchon-Dupeyrat, J. C. Garno, G. Y. Liu, G. K. Jennings, T. H. Yong, P. E. Laibinis, In situ studies of thiol self-assembly on gold from solution using atomic force microscopy, *J. Chem. Phys.* **108**, 5002–5012 (1998).
39. G. E. Poirier, E. D. Pylant, The self-assembly mechanism of alkanethiols on Au(111), *Science* **272**, 1145–1148 (1996).
40. G. E. Poirier, Mechanism of formation of Au vacancy islands in alkanethiol monolayers on Au(111), *Langmuir* **13**, 2019–2026 (1997).
41. T. T. Brown, Z. M. LeJeune, K. Liu, S. Hardin, J.-R. Li, K. Rupnik, J. C. Garno, Automated scanning probe lithography with *n*-alkanethiol self-assembled monolayers on Au(111): Application for teaching undergraduate laboratories, *J. Am. Lab Automat.*, **16**, 112–125 (2011).
42. S. Xu, N. A. Amro, G. Y. Liu, Characterization of AFM tips using nanografting, *Appl. Surf. Sci.* **175**, 649–655 (2001).
43. A.-S. Duwez, Exploiting electron spectroscopies to probe the structure and organization of self-assembled monolayers: A review, *J. Electron Spectrosc. Relat. Phenom.* **134**, 97–138 (2004).
44. P. Fenter, P. Eisenberger, K. S. Liang, Chain-length dependence of the structures and phases of ch3(ch2)n-1sh self-assembled on Au(111), *Phys. Rev. Lett.* **70**, 2447–2450 (1993).
45. R. G. Nuzzo, E. M. Korenic, L. H. Dubois, Studies of the temperature-dependent phase-behavior of long-chain normal-alkyl thiol monolayers on gold, *J. Chem. Phys.* **93**, 767–773 (1990).
46. M. D. Porter, T. B. Bright, D. L. Allara, C. E. D. Chidsey, Spontaneously organized molecular assemblies. 4. Structural characterization of normal-alkyl thiol monolayers on gold by optical ellipsometry, infrared-spectroscopy, and electrochemistry, *J. Am. Chem. Soc.* **109**, 3559–3568 (1987).
47. R. G. Nuzzo, B. R. Zegarski, L. H. Dubois, Fundamental-studies of the chemisorption of organosulfur compounds on Au(111) – implications for molecular self-assembly on gold surfaces, *J. Am. Chem. Soc.* **109**, 733–740 (1987).
48. T. L. Brower, J. C. Garno, A. Ulman, G. Y. Liu, C. Yan, A. Golzhauser, M. Grunze, Self-assembled multilayers of 4,4′-dimercaptobiphenyl formed by Cu(II)-catalyzed oxidation, *Langmuir* **18**, 6207–6216 (2002).

49. M. Kadalbajoo, J.-H. Park, A. Opdahl, H. Suda, J. C. Garno, J. D. Batteas, M. J. Tarlov, P. DeShong, Synthesis and structural characterization of glucopyranosylamide films on gold, *Langmuir* **23**, 700–707 (2007).
50. D. Liu, A. Bruckbauer, C. Abell, S. Balasubramanian, D.-J. Kang, D. Klenerman, D. Zhou, A reversible pH-driven DNA nanoswitch array, *J. Am. Chem. Soc.* **128**, 2067–2071 (2006).
51. J. t. Riet, T. Smit, M. J. J. Coenen, J. W. Gerritsen, A. Cambi, J. A. A. W. Elemans, S. Speller, C. G. Figdor, AFM topography and friction studies of hydrogen-bonded bilayers of functionalized alkanethiols, *Soft Matter* **6**, 3450–3454 (2010).
52. J. T. Riet, T. Smit, J. W. Gerritsen, A. Cambi, J. Elemans, C. G. Figdor, S. Speller, Molecular friction as a tool to identify functionalized alkanethiols, *Langmuir* **26**, 6357–6366 (2010).
53. W. J. Price, P. K. Kuo, T. R. Lee, R. Colorado, Z. C. Ying, G.-Y. Liu, Probing the local structure and mechanical response of nanostructures using force modulation and nanofabrication, *Langmuir* **21**, 8422–8428 (2005).
54. W. J. Price, S. A. Leigh, S. M. Hsu, T. E. Patten, G.-Y. Liu, Measuring the size dependence of Young′s modulus using force modulation atomic force microscopy, *J. Phys. Chem. A* **110**, 1382–1388 (2006).
55. D. Scaini, M. Castronovo, L. Casalis, G. Scoles, Electron transfer mediating properties of hydrocarbons as a function of chain length: A differential scanning conductive tip atomic force microscopy investigation, *ACS Nano* **2**, 507–515 (2008).
56. S. Xu, P. E. Laibinis, G. Y. Liu, Accelerating the kinetics of thiol self-assembly on gold – a spatial confinement effect, *J. Am. Chem. Soc.* **120**, 9356–9361 (1998).
57. J. J. Yu, Y. H. Tan, X. Li, P. K. Kuo, G. Y. Liu, A nanoengineering approach to regulate the lateral heterogeneity of self-assembled monolayers, *J. Am. Chem. Soc.* **128**, 11574–11581 (2006).
58. S. F. Chen, L. Y. Li, C. L. Boozer, S. Y. Jiang, Controlled chemical and structural properties of mixed self-assembled monolayers of alkanethiols on Au(111), *Langmuir* **16**, 9287–9293 (2000).
59. D. Hobara, T. Kakiuchi, Domain structure of binary self-assembled monolayers composed of 3-mercapto-1-propanol and 1-tetradecanethiol on Au(111) prepared by coadsorption *Electrochem. Commun.* **3**, 154–157 (2001).
60. S. Ryu, G. C. Schatz, Nanografting: Modeling and simulation, *J. Am. Chem. Soc.* **128**, 11563–11573 (2006).
61. J. Liang, L. G. Rosa, G. Scoles, Nanostructuring, imaging and molecular manipulation of dithiol monolayers on Au(111) surfaces by atomic force microscopy, *J. Phys. Chem C* **111**, 17275–17284 (2007).
62. J. F. Liu, S. Cruchon-Dupeyrat, J. C. Garno, J. Frommer, G. Y. Liu, Three-dimensional nanostructure construction via nanografting: Positive and negative pattern transfer, *Nano Lett.* **2**, 937–940 (2002).
63. J. M. Lim, Z. S. Yoon, J. Y. Shin, K. S. Kim, M. C. Yoon, D. Kim, The photophysical properties of expanded porphyrins: Relationships between aromaticity, molecular geometry and non-linear optical properties, *Chem. Commun.* **3**, 261–273 (2009).
64. T. Hasobe, Supramolecular nanoarchitectures for light energy conversion, *Phys. Chem. Chem. Phys.* **12**, 44–57 (2010).
65. Z. M. LeJeune, M. E. McKenzie, E. Hao, M. G. H. Vicente, B. Chen, J. C. Garno, Self-assembly of pyridyl-substituted porphyrins investigated in situ using AFM, *Abstracts Am. Chem. Soc.* **235**, 216-COLL (2008).
66. R. G. Chapman, E. Ostuni, S. Takayama, R. E. Holmlin, L. Yan, G. M. Whitesides, Surveying for surfaces that resist the adsorption of proteins, *J. Am. Chem. Soc.* **122**, 8303–8304 (2000).
67. E. Ostuni, R. G. Chapman, M. N. Liang, G. Meluleni, G. Pier, D. E. Ingber, G. M. Whitesides, Self-assembled monolayers that resist the adsorption of proteins and the adhesion of bacterial and mammalian cells, *Langmuir* **17**, 6336–6343 (2001).

68. R. E. Holmlin, X. Chen, R. G. Chapman, S. Takayama, G. M. Whitesides, Zwitterionic sams that resist nonspecific adsorption of protein from aqueous buffer, *Langmuir* **17**, 2841–2850 (2001).
69. E. Ostuni, R. G. Chapman, R. E. Holmlin, S. Takayama, G. M. Whitesides, A survey of structure-property relationships of surfaces that resist the adsorption of protein, *Langmuir* **17**, 5605–5620 (2001).
70. Y.-Y. Luk, M. Kato, M. Mrksich, Self-assembled monolayers of alkanethiolates presenting mannitol groups are inert to protein adsorption and cell attachment, *Langmuir* **16**, 9604–9608 (2000).
71. S. Herrwerth, W. Eck, S. Reinhardt, M. Grunze, Factors that determine the protein resistance of oligoether self-assembled monolayers – internal hydrophilicity, terminal hydrophilicity, and lateral packing density, *J. Am. Chem. Soc.* **125**, 9359–9366 (2003).
72. Z. Grabarek, J. Gergely, Zero-length crosslinking procedure with the use of active esters, *Anal. Biochem.* **185**, 131–135 (1990).
73. D. J. Zhou, X. Z. Wang, L. Birch, T. Rayment, C. Abell, AFM study on protein immobilization on charged surfaces at the nanoscale: Toward the fabrication of three-dimensional protein nanostructures, *Langmuir* **19**, 10557–10562 (2003).
74. J. R. Kenseth, J. A. Harnisch, V. W. Jones, M. D. Porter, Investigation of approaches for the fabrication of protein patterns by scanning probe lithography, *Langmuir* **17**, 4105–4112 (2001).
75. C.-H. Jang, B. D. Stevens, R. Phillips, M. A. Calter, W. A. Ducker, A strategy for the sequential patterning of proteins: Catalytically active multiprotein nanofabrication, *Nano Lett.* **3**, 691–694 (2003).
76. C. Staii, D. W. Wood, G. Scoles, Verification of biochemical activity for proteins nanografted on gold surfaces, *J. Am. Chem. Soc.* **130**, 640–646 (2007).
77. M. Castronovo, S. Radovic, C. Grunwald, L. Casalis, M. Morgante, G. Scoles, Control of steric hindrance on restriction enzyme reactions with surface-bound DNA nanostructures, *Nano Lett.* **8**, 4140–4145 (2008).
78. M. Liu, G.-Y. Liu, Hybridization with nanostructures of single-stranded DNA, *Langmuir* **21**, 1972–1978 (2005).
79. P. V. Schwartz, Meniscus force nanografting: Nanoscopic patterning of DNA, *Langmuir* **17**, 5971–5977 (2001).
80. E. Mirmomtaz, M. Castronovo, C. Grunwald, F. Bano, D. Scaini, A. A. Ensafi, G. Scoles, L. Casalis, Quantitative study of the effect of coverage on the hybridization efficiency of surface-bound DNA nanostructures, *Nano Lett.* **8**, 4134–4139 (2008).
81. F. Bano, L. Fruk, B. Sanavio, M. Glettenberg, L. Casalis, C. M. Niemeyer, G. Scoles, Toward multiprotein nanoarrays using nanografting and DNA directed immobilization of proteins, *Nano Lett.* **9**, 2614–2618 (2009).
82. E. A. Josephs, T. Ye, Nanoscale positioning of individual DNA molecules by an atomic force microscope, *J. Am. Chem. Soc.* **132**, 10236–10238 (2010).
83. M. V. Lee, K. A. Nelson, L. Hutchins, H. A. Becerril, S. T. Cosby, J. C. Blood, D. R. Wheeler, R. C. Davis, A. T. Woolley, J. N. Harb, M. R. Linford, Nanografting of silanes on silicon dioxide with applications to DNA localization and copper electroless deposition, *Chem. Mater.* **19**, 5052–5054 (2007).
84. M. Despont, U. Drechsler, U. Durig, W. Haberle, M. I. Lutwyche, H. E. Rothuizen, R. Stutz, R. Widmer, G. Binnig, The "Millipede" – more than one thousand tips for future AFM data storage, *IBM J. Res. Dev.* **44**, 323–340 (2000).
85. K. Salaita, Y. Wang, J. Fragala, R. A. Vega, C. Liu, C. A. Mirkin, Massively parallel dip-pen nanolithography with 55,000-pen two-dimensional arrays, *Angew. Chem. Int. Ed.* **45**, 7220–7223 (2007).
86. J.-J. Yu, J. N. Ngunjiri, A. T. Kelley, J. C. Garno, Nanografting versus solution self-assembly of α, ω-alkanedithiols on Au(111) investigated by AFM, *Langmuir* **24**, 11661–11668 (2008).

87. C. H. Jang, B. D. Stevens, R. Phillips, M. A. Calter, W. A. Ducker, A strategy for the sequential patterning of proteins: Catalytically active multiprotein nanofabrication, *Nano Lett.* **3**, 691–694 (2003).
88. N. Nuraje, I. A. Banerjee, R. I. MacCuspie, L. T. Yu, H. Matsui, Biological bottom-up assembly of antibody nanotubes on patterned antigen arrays, *J. Am. Chem. Soc.* **126**, 8088–8089 (2004).
89. C. Staii, D. W. Wood, G. Scoles, Ligand-induced structural changes in maltose binding proteins measured by atomic force microscopy, *Nano Lett.* **8**, 2503–2509 (2008).
90. I. Kopf, C. Grunwald, E. Brundermann, L. Casalis, G. Scoles, M. Havenith, Detection of hybridization on nanografted oligonucleotides using scanning near-field infrared microscopy, *J. Phys. Chem. C* **114**, 1306–1311 (2010).